

AD-A150 429

CONTROL OF CASCADED INDUCTION GENERATOR SYSTEMS(U)

1/1

CLARKSON COLL OF TECHNOLOGY POTSDAM NY DEPT OF

ELECTRICAL AND COMPUTER ENGINEERING T H ORTMEYER

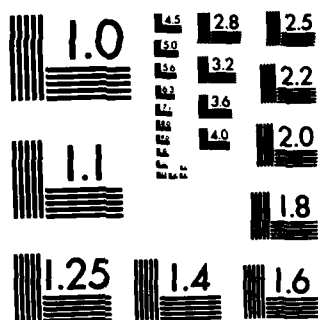
UNCLASSIFIED

13 DEC 84 AFOSR-TR-84-1259 AFOSR-83-0268

F/G 10/2

NL

									END				
									FORMED				
									DATE				



MICROCOPY RESOLUTION TEST CHART
NATIONAL BUREAU OF STANDARDS-1963-A

UNCLASSIFIED

SECURITY CLASSIFICATION OF THIS PAGE (When Data Entered)

REPORT DOCUMENTATION PAGE		READ INSTRUCTIONS/ BEFORE COMPLETING FORM
1. AFOSR-TR-84-1259 Annual Technical Report	2. GOVT ACCESSION NO.	3. RECIPIENT'S CATALOG NUMBER
4. TITLE (and Subtitle) Control of Cascaded Induction Generator Systems	5. TYPE OF REPORT & PERIOD COVERED 9/1/83 - 8/30/84 Final Technical <i>Final</i>	6. PERFORMING ORG. REPORT NUMBER Annual Technical
7. AUTHOR(s) Thomas H. Ortmeier	8. CONTRACT OR GRANT NUMBER(s) AFOSR AFOSR -83-0268	9. PROGRAM ELEMENT, PROJECT, TASK AREA & WORK UNIT NUMBERS 61102F 2305/09
10. PERFORMING ORGANIZATION NAME AND ADDRESS Clarkson University Department of Electrical and Computer Eng. Potsdam, NY 13676	11. CONTROLLING OFFICE NAME AND ADDRESS AFOSR/NE Building 410 Bolling AFB, DC 20332	12. REPORT DATE 12/13/84
13. MONITORING AGENCY NAME & ADDRESS (if different from Controlling Office)	14. NUMBER OF PAGES UNCLASSIFIED	15. SECURITY CLASS. (of this report) UNCLASSIFIED
16. DISTRIBUTION STATEMENT (of this Report) Approved for public release; distribution unlimited.		17. DECLASSIFICATION/DOWNGRADING SCHEDULE

AD-A150 429

DTIC FILE COPY

17. DISTRIBUTION STATEMENT (of the abstract entered in Block 20, if different from Report)

18. SUPPLEMENTARY NOTES

19. KEY WORDS (Continue on reverse side if necessary and identify by block number)

20. ABSTRACT (Continue on reverse side if necessary and identify by block number)

This report documents an investigation of the stability and control of cascaded doubly fed machines (CDFM). These machines are brushless variable speed constant frequency electric power generators with potential for application in aircraft.

85 01 31 018

DD FORM 1 JAN 73 1473

EDITION OF 1 NOV 68 IS OBSOLETE

UNCLASSIFIED

SECURITY CLASSIFICATION OF THIS PAGE (When Data Entered)

SECURITY CLASSIFICATION OF THIS PAGE(When Data Entered)

Step 1 results show that the machines exhibit stability characteristics in the supersynchronous mode similar to those observed in the subsynchronous mode. Step 2 results show that output capacitors degrade the system performance, particularly at light loads. The results show that output current feedback can be employed to improve the system performance.

ORIG
COPY
INSPECTED
3

SECURITY CLASSIFICATION OF THIS PAGE (When Data Entered)

AFOSR-TR- 84 - 1259

Control of Cascaded Induction Generator Systems

Annual Technical Report

By

T.H. Ortmeier

Department of Electrical and Computer Engineering

Clarkson University

Potsdam, New York 13676

**Approved for public release;
distribution unlimited.**

INTRODUCTION

Cascaded doubly fed machines have been shown to have potential for application in aircraft electric power systems. An initial investigation of the steady state performance of these machines [1] predicted their ability to perform as a brushless variable speed constant frequency generator, with competitive weight and cost and the potential for high reliability.

The basic system layout is shown in Figure 1. The machines have multi-phase AC windings on both the stator and rotor. Excitation for the main machine rotor is provided by the exciting machine. The stator of the exciting machine is supplied by a solid state power converter connected to a shaft driven permanent magnet machine, which provides stand alone capability. As direct currents cannot be induced onto the rotor, the main machine must be operated strictly above or below synchronous speed. When using conventional machine analysis during supersynchronous operation, negative frequencies occur [2]. These negative frequencies complicate the analysis of the supersynchronous operating mode. An investigation of machine stability in the subsynchronous operating mode [3] showed that the machine damping could be improved by feedback of the field currents to simulate an increased field resistance. With the analytical model used, the resistance simulation provided stability and good response. Subsequent laboratory tests of the steady state [4] and dynamic state [5] have shown the validity of the analysis.

The purpose of this project has been to analyze the dynamic operation of the machines to provide understanding in two particular areas: first, the machine characteristics in supersynchronous operation; and secondly, the affect of capacitance connected at the machine output on the dynamic performance. The report is divided into two main sections which represent these two goals. Each

section begins with a derivation of the model required for the analysis. In both cases, the model was used for linearized analysis and nonlinear time domain simulation. The results acquired from the analysis and resulting conclusions, are presented in each section. The final computer programs are listed in the appendix, with brief descriptions.

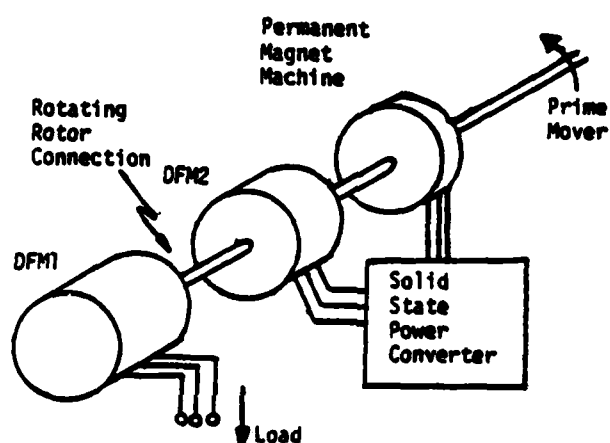


Figure 1. Stand-alone brushless variable speed constant frequency generator system using doubly fed (DFM).

Step 1: Supersynchronous Operation.

a) Analysis

The analysis of the two doubly fed machines is based on the two axis theory of machines [6]. The definitions for the reference frames for each machine are shown in Figure 2. In this figure, the main, or output, machine is designated as machine M1, and the exciting machine is designated as M2. The reference frame speed is defined as

$$p\Theta = \omega_e = \text{nominal output frequency, electrical rad/sec} \quad (1)$$

with respect to the stator magnetic axis. $p(\cdot)$ is defined as the derivative operator $d(\cdot)/dt$, ω_e is the synchronous speed of this machine. The stator transformation from three phase quantities to axis quantities

$$P_s = \sqrt{\frac{2}{3}} \begin{bmatrix} 1/\sqrt{2} & 1/\sqrt{2} & 1/\sqrt{2} \\ \cos\theta & \cos(\theta - \frac{2\pi}{3}) & \cos(\theta + \frac{2\pi}{3}) \\ -\sin\theta & -\sin(\theta - \frac{2\pi}{3}) & -\sin(\theta + \frac{2\pi}{3}) \end{bmatrix} \quad (2)$$

Similarly, rotor transformation is P_r . The resulting machine equations are:

$$\begin{aligned} v_{ds} &= r_s i_{ds} + p\lambda_{ds} - \omega_e \lambda_{qs} \\ v_{qs} &= r_s i_{qs} + p\lambda_{qs} + \omega_e \lambda_{ds} \\ v_{dr} &= r_r i_{dr} + p\lambda_{dr} - (\omega_e - \omega_r) \lambda_{qr} \\ v_{qr} &= r_r i_{qr} + p\lambda_{qr} + (\omega_e - \omega_r) \lambda_{dr} \end{aligned}$$

where

$$\begin{aligned} \lambda_{ds} &= L_s i_{ds} + L_m i_{dr} \\ \lambda_{qs} &= L_s i_{qs} + L_m i_{qr} \\ \lambda_{dr} &= L_r i_{dr} + L_m i_{ds} \\ \lambda_{qr} &= L_r i_{qr} + L_m i_{qs} \end{aligned}$$

During normal steady state operation, the machine output frequency is ω_e radians per second, and the rotor frequency, or slip frequency is

$$p\beta = \omega_s \quad \text{radians/second} \quad (5)$$

In this case, the stator and rotor axis voltages and currents are slowly

changing quantities with constant steady state values. The rotor speed is

$$\omega_r = \frac{P_1}{2} \omega_m = \dot{\alpha} \quad (6)$$

where P_1 is the number of poles of machine 1. Therefore, the slip frequency is

$$\omega_s = \omega_e - \omega_r \quad (7)$$

with ω_s being positive for subynchronous operation and negative for supersynchronous operation.

As the armature of M2 is on the rotor, the primary reference point for the d and q axis is the rotor winding. The armature electrical frequency, rotor speed, and slip frequency are

$$\begin{aligned} \omega_{e2} &= \dot{\eta} \\ \omega_{r2} &= \frac{P_2}{2} \omega_m = \dot{\gamma} \end{aligned} \quad (8)$$

$$\omega_{s2} = \omega_{e2} - \omega_{r2} = \dot{\epsilon}$$

all in electrical radians per second. The angle definitions are given in Figure 2, and P_2 is the number of poles of machine 2. The phase axis transformations for this machine are P_η and P_ϵ for the armature and field, respectively, and the electrical quantities are slowly changing variables when the conditions of Eq. 8 are observed.

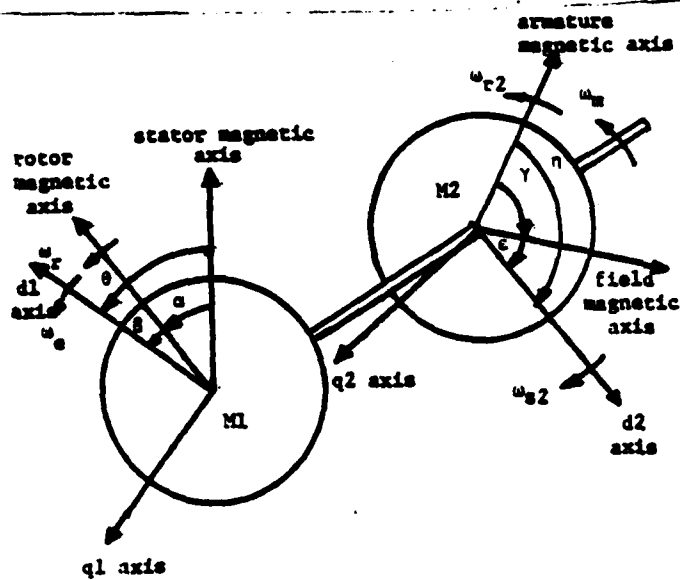


Figure 2. d and q axis reference frame definitions for doubly fed machines M1 and M2.

The resulting machine 2 equations are:

$$\begin{aligned}
 v_{dA} &= r_A i_{dA} + p \lambda_{dA} - \omega_{e2} \lambda_{qA} \\
 v_{qA} &= r_A i_{qA} + p \lambda_{qA} + \omega_{e2} \lambda_{dA} \\
 v_{dF} &= r_F i_{dF} + p \lambda_{dF} - (\omega_{e2} - \omega_{r2}) \lambda_{qF} \\
 v_{qF} &= r_F i_{qF} + p \lambda_{qF} + (\omega_{e2} - \omega_{r2}) \lambda_{dF}
 \end{aligned} \tag{9}$$

where

$$\begin{aligned}
 \lambda_{dA} &= L_A i_{dA} + L_{am} i_{dF} \\
 \lambda_{qA} &= L_A i_{qA} + L_{am} i_{qF} \\
 \lambda_{dF} &= L_F i_{dF} + L_{am} i_{dA} \\
 \lambda_{qF} &= L_F i_{qF} + L_{am} i_{qA}
 \end{aligned} \tag{10}$$

There exist two independent connections between the phase windings of the rotor of M1 and the rotor of M2. The first of these is

$$\begin{bmatrix} v_{ar} \\ v_{br} \\ v_{cr} \end{bmatrix} = \begin{bmatrix} v_{aA} \\ v_{bA} \\ v_{cA} \end{bmatrix} \begin{bmatrix} i_{ar} \\ i_{br} \\ i_{cr} \end{bmatrix} = \begin{bmatrix} -i_{aA} \\ -i_{bA} \\ -i_{cA} \end{bmatrix} \tag{11}$$

and the rotor reference frame angles are defined as

$$\beta = \gamma \tag{12}$$

In this case, the d and q axis quantities are

$$\begin{bmatrix} v_{dr} \\ v_{qr} \end{bmatrix} = \begin{bmatrix} v_{dA} \\ v_{qA} \end{bmatrix} \quad (13)$$

$$\begin{bmatrix} i_{dr} \\ i_{qr} \end{bmatrix} = - \begin{bmatrix} i_{dA} \\ i_{qA} \end{bmatrix}$$

This connection is practical only for subsynchronous operation.

The a phase connection can be assumed to be the same for the second type of connection.

$$\begin{bmatrix} v_{ar} \\ v_{br} \\ v_{cr} \end{bmatrix} = \begin{bmatrix} v_{aA} \\ v_{cA} \\ v_{bA} \end{bmatrix}, \quad \begin{bmatrix} i_{ar} \\ i_{br} \\ i_{cr} \end{bmatrix} = \begin{bmatrix} -i_{aA} \\ -i_{cA} \\ -i_{bA} \end{bmatrix} \quad (14)$$

With reference frame definition

$$\beta = -\pi \quad (15)$$

the d and q axis equations will be

$$\begin{bmatrix} v_{dr} \\ v_{qr} \end{bmatrix} = \begin{bmatrix} v_{dA} \\ -v_{qA} \end{bmatrix}, \quad \begin{bmatrix} i_{dr} \\ i_{qr} \end{bmatrix} = \begin{bmatrix} -i_{dA} \\ i_{qA} \end{bmatrix} \quad (16)$$

This second type of connection is practical only for the supersynchronous operating mode. Note that ω_{e2} is positive for all practical operating conditions. These connections are practical as they minimize the ratio of field power to output power.

Assuming that the practical connection is used for each mode, Equations 13 and 16 can be written as

$$\begin{aligned} v_{dr} &= v_{dA} \\ i_{dr} &= -i_{dA} \\ v_{qr} &= C_s v_{qR} \\ i_{qr} &= -C_s i_{qA} \end{aligned} \quad (17)$$

where

$$\begin{aligned} C_s &= 1 \text{ subsynchronous operation} \\ &= -1 \text{ supersynchronous operation} \end{aligned} \quad (18)$$

By interconnecting the rotor windings, two constraints are placed on the system, and two of the eight equations in (3) and (9) must be eliminated. By combining the rotor equations and maintaining i_{dr} and i_{qr} as state variables, the system equations become:

$$\begin{aligned} v_{ds} &= r_s i_{ds} + L_s p i_{ds} + L_m p i_{dr} - \omega_e (L_s i_{qs} + L_m i_{qr}) \\ v_{qs} &= r_s i_{qs} + L_s p i_{qs} + L_m p i_{qr} + \omega_e (L_s i_{ds} - L_m i_{dr}) \\ 0 &= (r_r + r_A) i_{dr} + (L_r + L_A) p i_{dr} + L_m p i_{ds} - L_{Am} p i_{df} \\ &\quad - \omega_s L_m i_{qs} - \omega_s (L_r + L_A) i_{qr} + \omega_{e2} L_{Am} i_{qf} \\ 0 &= (r_r + r_A) i_{qr} + (L_r + L_A) p i_{qr} + L_m p i_{qs} - C_s L_{Am} p i_{qf} \\ &\quad + \omega_s [L_m i_{ds} + (L_r + L_A) i_{dr} - L_{Am} i_{df}] \\ v_{df} &= r_f i_{df} + L_f p i_{df} - L_{Am} p i_{dr} - \omega_{e2} (L_f i_{qf} - C_s L_{Am} i_{qr}) \\ v_{qf} &= r_f i_{qf} + L_f p i_{qf} - C_s L_{Am} p i_{qr} + \omega_{e2} (L_f i_{df} - L_{Am} i_{dr}) \end{aligned} \quad (19)$$

This set of equations is valid for either subsynchronous or supersynchronous operation. Existing programs for eigenvalue and time simulation were upgraded to include these equations.

The programs assume that the field voltage is aligned with the d_2 axis. The specification of initial conditions is done in terms of output terminal quantities (voltage, current power, and frequency) as well as machine speed. This requires the definition of x_1 and y_1 axes for machine 1 and x_2 and y_2 axes for machine 2 which are displaced from the d_1 and d_2 axes by some constant angle. The initial state problem is solved by setting the output voltage on the x_1 axis, solving for the rotor and field currents, and then reflecting these quantities to the d_1 , d_2 , q_1 and q_2 axes.

The linearized analysis program and the simulation program were developed from this analysis and verified by comparison of solution between the programs.

b) Resistance simulation

Previous studies of subsynchronous operation [3,5] had shown that stability could be provided by feedback of the field currents to simulate increased resistance in the field circuit, thereby providing damping to the system. The feedback equations are

$$\begin{bmatrix} v_{df} \\ v_{qf} \end{bmatrix} = \begin{bmatrix} v_{ds} \\ 0 \end{bmatrix} - \begin{bmatrix} C_1 & 0 \\ 0 & C_1 \end{bmatrix} \begin{bmatrix} i_{df} \\ i_{qf} \end{bmatrix} \quad (20)$$

v_{df} and v_{qf} are the actual field voltage commands sent to the power converter, and v_{ds} is the simulated field voltage. The output voltage is regulated by an integral controller. The basic controller is shown in Figure 3. With assumptions of ideal current and voltage sensing, and an ideal power converter, the feedback quantity C_1 exactly represents increased field resistance. These assumptions are employed in this analysis.

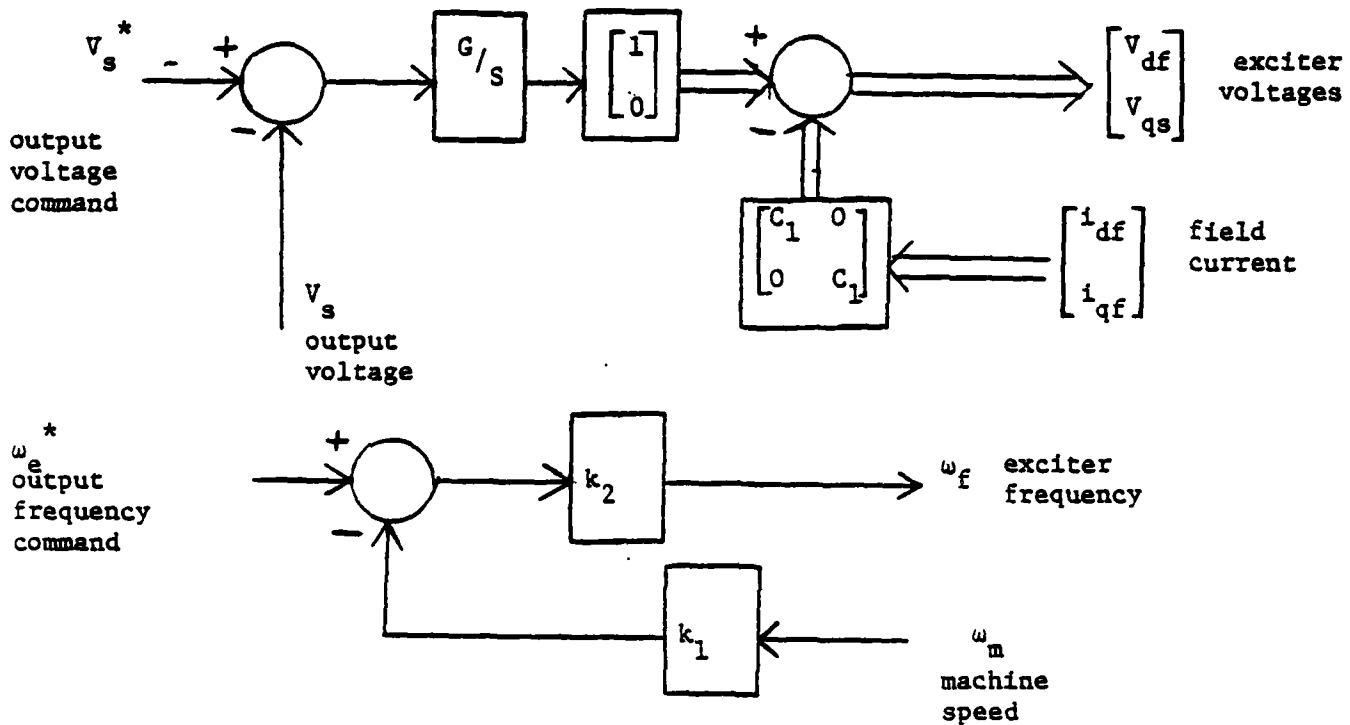


Figure 3. Basic system controller with state feedback of the machine field currents.

C) Results

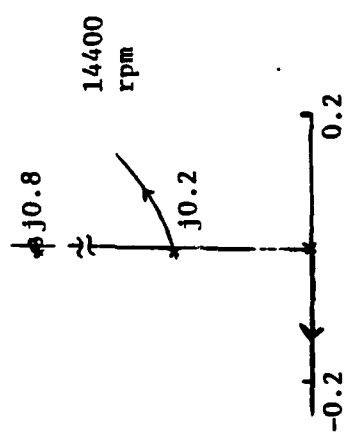
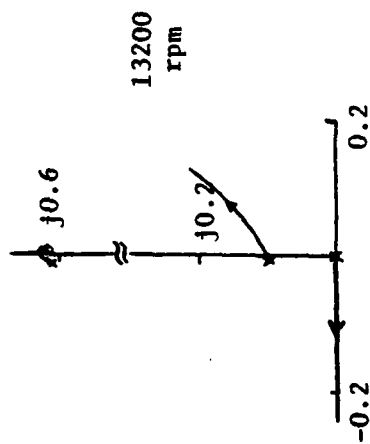
The model given in parts a and b of this section was used to study the controllability of the machines in supersynchronous operation. As the machine control during subsynchronous operation was previously studied, a comparison between these two modes was indicated. For this comparison, the machine constants given in Table I were used. For both the sub- and supersynchronous cases. The cases involve identical machines run over 1.5:1 speed ranges.

The root loci for the machines are given in Figures 4 and 5. These figures show the significant loci in the upper half of the s -plane. Both modes of operation exhibit a complex pole-zero pair, with relatively close coupling of this pole and zero. This pair is associated with the rotor winding of the machines. The second complex pole-zero pair which is shown is related to the field winding of the machines. Figure 4 compares sub- and supersynchronous operation with no state feedback. In all cases, the open loop poles are lightly damped. At low speeds, both cases exhibit a zero in the RHP near the $j\omega$ axis. At high speeds, both systems exhibit a zero far into the RHP. Figure 5 contains the results with resistance simulation feedback $c_1 = 59r_f$. As is true in subsynchronous operation, the feedback successfully moves the open loop pole of the system into the LHP. Additionally, close coupling between the rotor pole-zero pair is obtained. At low speeds, the zero associated with the field is located in the LHP and the system is stable for all integrator gains. As the speed increases, this zero moves into the RHP, and the system becomes unstable at high gain. Figure 5 shows that this movement of the zero occurs at a relatively lower speed in supersynchronous operation than in subsynchronous operation. At the highest speed in subsynchronous operation, the rotor zero moves above the open loop pole, and the field locus crosses the $j\omega$ axis below the rotor pole-zero pair. These events also lead to degraded performance at high gain.

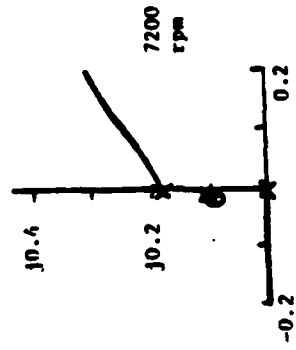
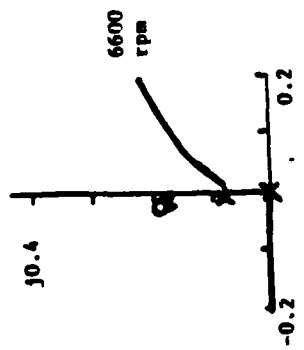
TABLE I

MACHINE CONSTANTS FOR 40 KVA, 400 HERTZ
GENERATOR, SUPERSYNCHRONOUS 9600-14400 rpm
SPEED RANGE. PER UNIT VALUES GIVEN ARE THE
MACHINE BASE.

	Machine 1	Machine 2
kVA	40.0	16.0
poles	6	2
frequency, hz	400	160
stator resistance	0.02 pu	0.025 pu
stator reactance	4.08 pu	4.08 pu
rotor resistance	0.025 pu	0.02 pu
rotor reactance	4.08 pu	4.08 pu
magnetizing reactance	4.0 pu	4.0 pu



b. supersynchronous operation



a. subsynchronous operation

Figure 4. Comparison of sub- and supersynchronous root loci with no state feedback. Rated output voltage and frequency with loading of 1% of rated power, unity power factor.

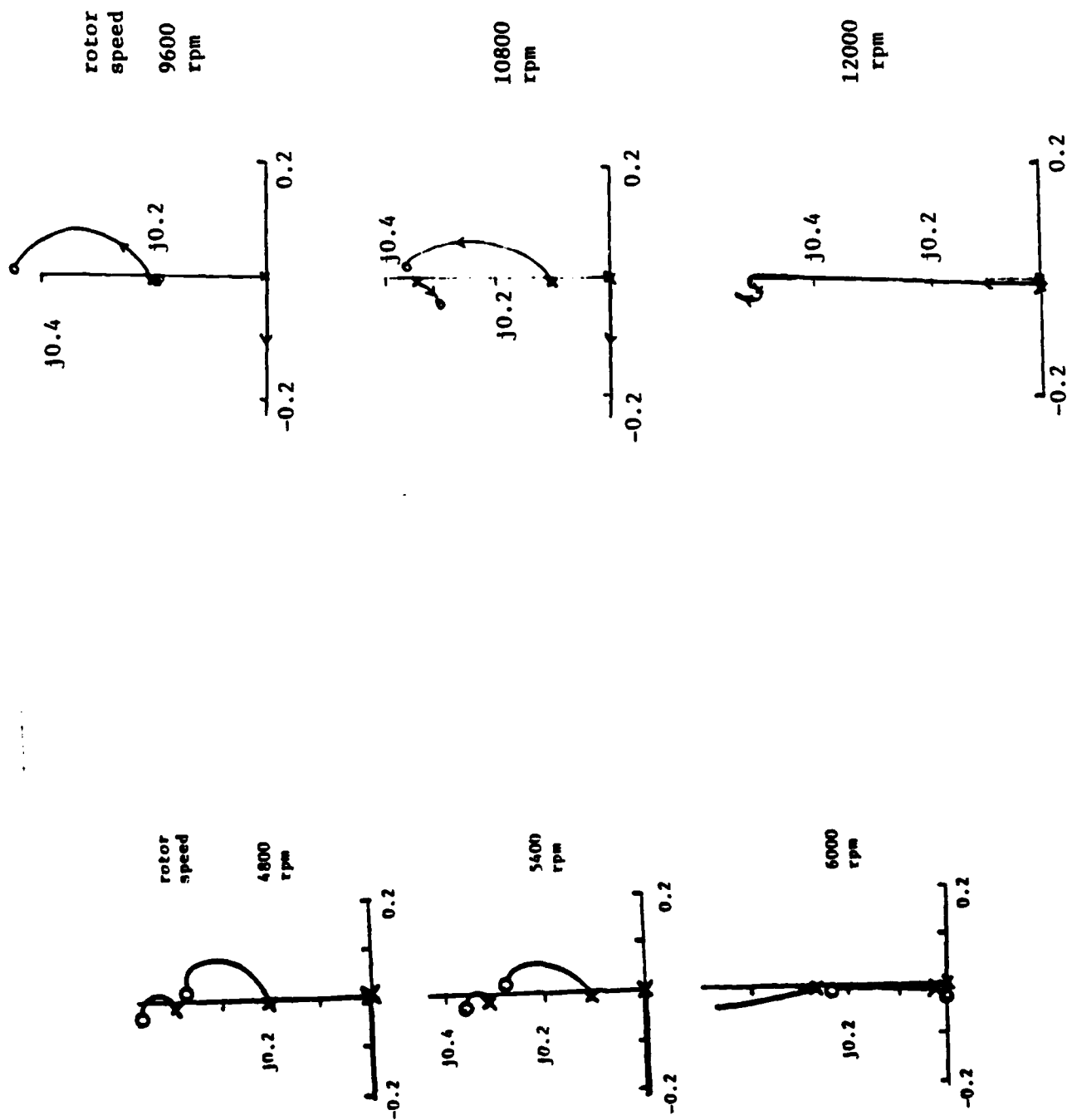
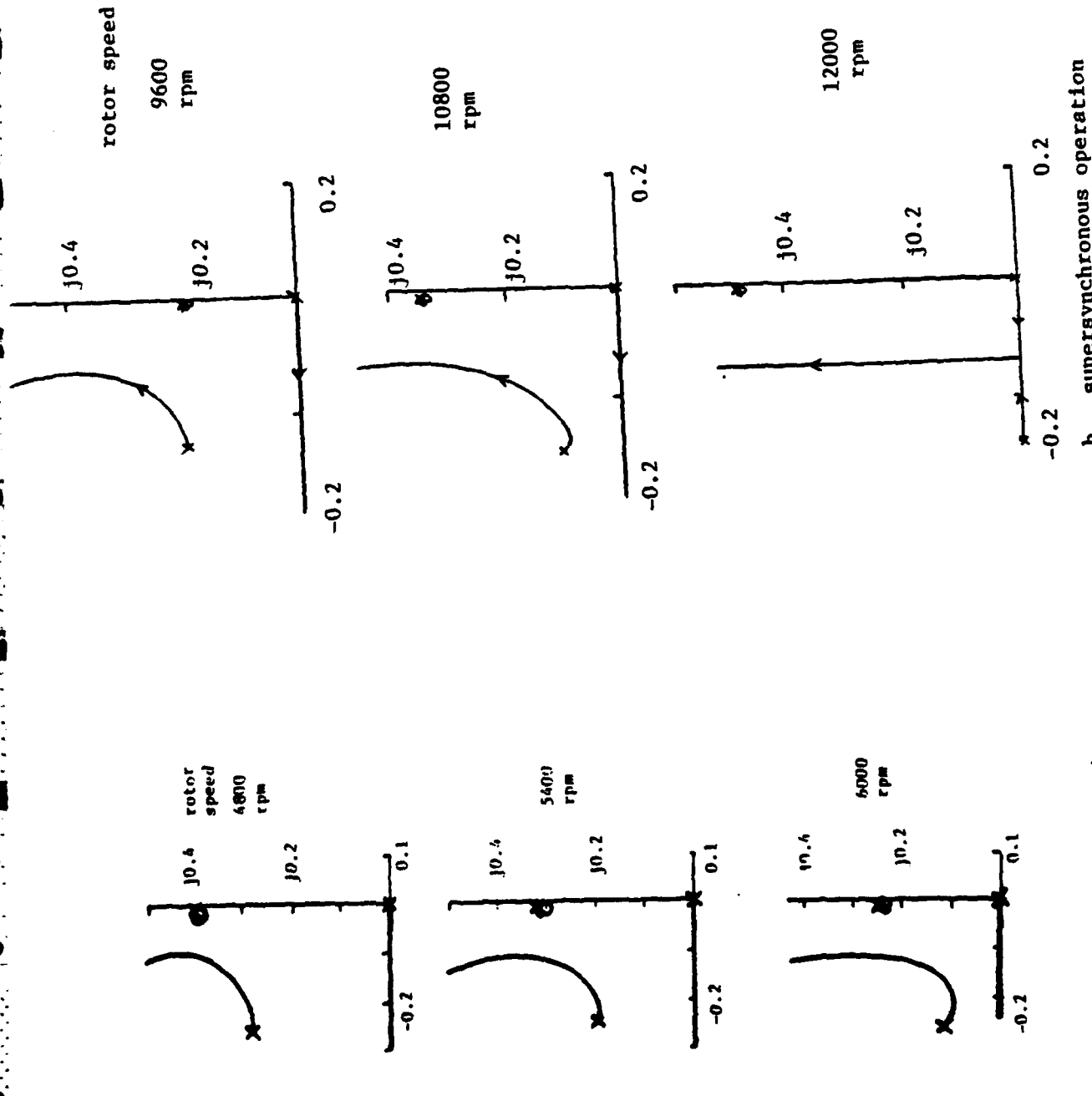


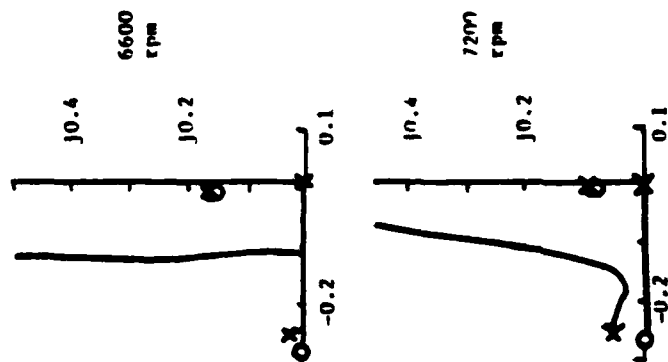
Figure 4. Continued



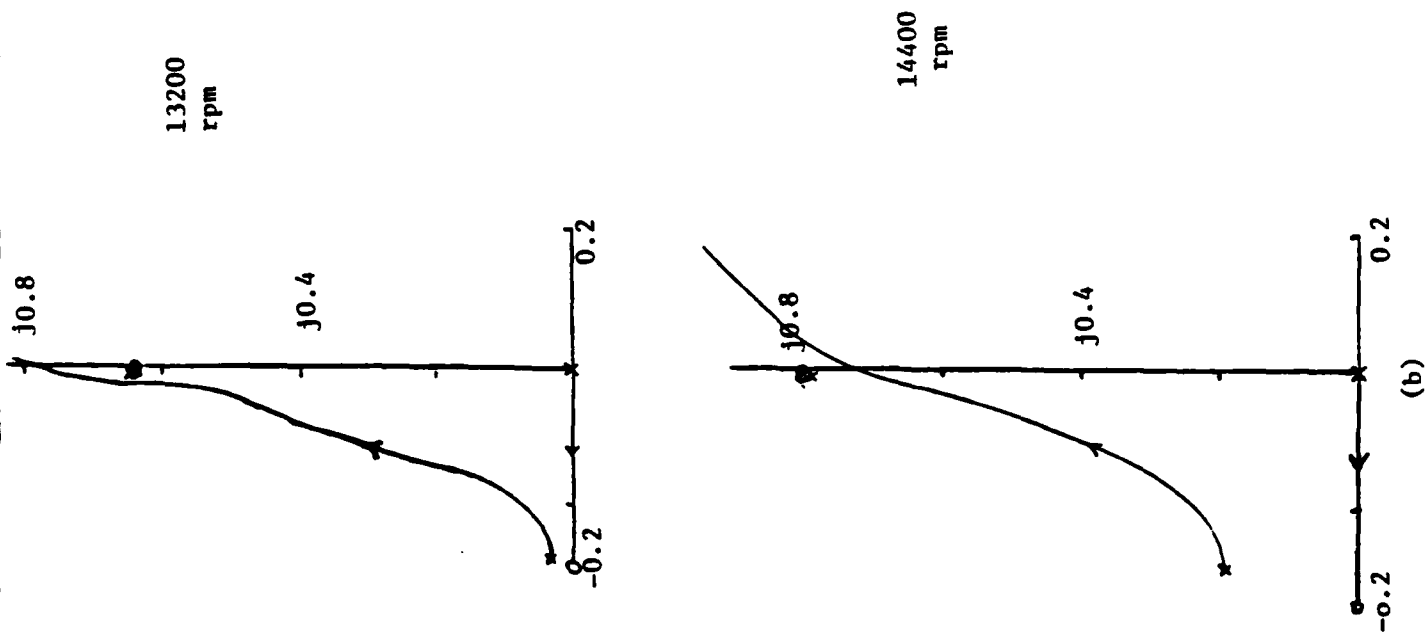
a. subsynchronous operation

b. supersynchronous operation

Figure 5. Comparison of sub- and supersynchronous root loci with state feedback of field currents, $C_1 = 59r_f$. Rated output voltage and frequency with loading of 1% of rated power, unity power factor.



(a)



(b)

The results show that stability can be obtained by implementing resistance simulation in both the subsynchronous and supersynchronous operating modes. For the case studied, sufficient damping was obtained throughout the speed range of interest to ensure good response. The subsynchronous mode showed slightly better characteristics at high speed, however, and it is possible that the subsynchronous mode could out perform the supersynchronous mode in cases involving a larger speed range. As the advantages of the cascade machine system are most pronounced where small speed ranges are required, and it appears that the sub- and supersynchronous modes of operation are equally controllable for low speed ranges.

Step 2: CDFM controllability with capacitive load

a) Analysis

The initial studies of the cascaded doubly fed machine (CDFM) generator system involved a passive series RL load on the generator. In many applications, however, it would be desirable to place shunt capacitors at the generator terminals to supply the load VARS and a share of the generator system excitation requirements. This would reduce the current flow in the exciter and field.

Step 2 of this project involves a study of the effect of this capacitance on machine stability. The system diagram is shown in Figure 6. The study involves shunt capacitance permanently connected at the generator terminals which supply VARS equal to 66% of the generator rating. The capacitors are permanently connected to the generator to avoid the weight and reliability problems of a switch. The bank rating was chosen from steady state considerations.

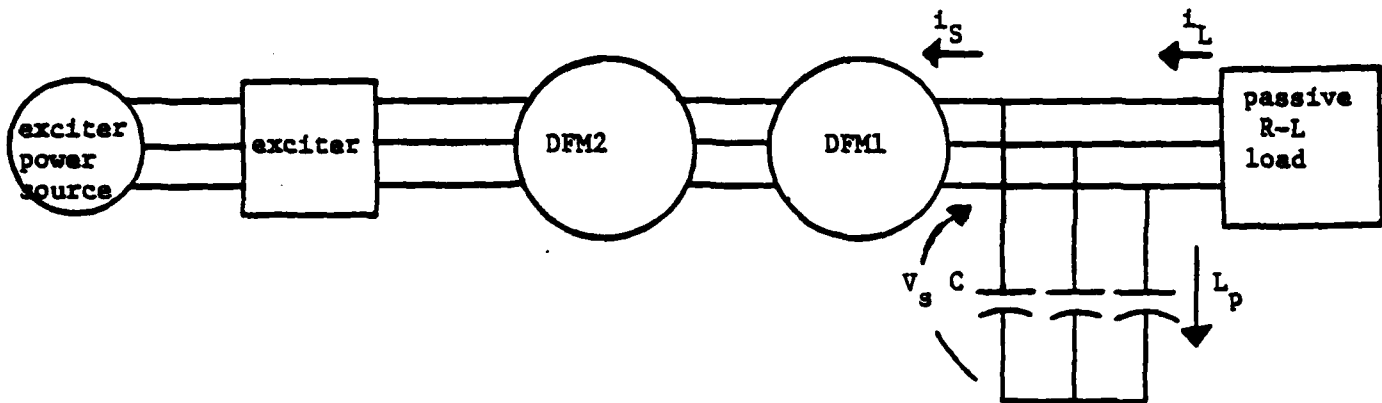


Figure 6. System diagram of the CDFM generator with capacitance supplying excitation VARS. Reference directions for the currents and voltages at the generator output are shown.

The addition of the capacitors will increase the state of the system by four: two for the capacitors and two for the load. The capacitor equations are:

$$\begin{bmatrix} i_{ap} \\ i_{bp} \\ i_{cp} \end{bmatrix} = C \begin{bmatrix} p v_{as} \\ p v_{bs} \\ p v_{cs} \end{bmatrix} \quad (21)$$

and the load equation are:

$$\begin{bmatrix} v_{as} \\ v_{bs} \\ v_{cs} \end{bmatrix} = L_L \begin{bmatrix} p i_{aL} \\ p i_{bL} \\ p i_{cL} \end{bmatrix} + R_L \begin{bmatrix} i_{aL} \\ i_{bL} \\ i_{cL} \end{bmatrix} \quad (22)$$

When these are transformed by the output winding transformation (Equation 2), the system equations are (neglecting the 0 axis quantities):

$$v_{ds} + R_L i_{dL} + L_L p i_{dL} - \omega_e L_L i_{qL} = 0 \quad (23)$$

$$v_{qs} + R_L i_{qL} + L_L p i_{qL} + \omega_e L_L i_{dL} = 0$$

$$i_{dp} = i_{dL} - i_{ds} = C p v_{ds} - \omega_e C v_{qs} \quad (24)$$

$$i_{qp} = i_{qL} - i_{qs} = C p v_{qs} + \omega_e C v_{ds}$$

where i_{dL} , i_{qL} , v_{ds} and v_{qs} have been chosen as the new state variables. The incremental magnitude of the output voltage is:

$$v_{ol} = \frac{v_{dso}}{v_{so}} v_{ds1} + \frac{v_{qso}}{v_{so}} v_{qs1} \quad (25)$$

The initial condition calculations are performed in the same manner as in step 1. The computer programs used to study the system are listed in the appendix. The results are presented in terms of linearized s-plane plots. The time simulation programs were used to validate these results. It has been found that

the system exhibits good time response when the real eigenvalue and the two dominant complex pairs all have negative real parts with magnitude greater than 0.1 pu. The lightly damped pole-zero pair remains closely coupled with the feedback strategies shown, and has negligible effect on the system response.

b) Results - field current feedback

The machines described in Table 1 were used to investigate the effect of output capacitors on system stability. Due to the results of step 1 of the project, only the subsynchronous operating mode was considered.

Figure 7 shows a root locus study of the system with voltage regulator but no state feedback. The dominant poles of the system are shown on the upper half of the per unit s-plane. The system is open loop unstable at the two upper speeds. At low speed, a lightly damped low frequency pole quickly goes into the RHP as controller gain is increased.

Field current feedback for resistance simulation was investigated. The results show that a level of resistance simulation somewhat higher than that employed in step 1 of the research will be effective in stabilizing a loaded system. Figure 8 shows the root locus plot with resistance simulation $C_1 = 2.0$ pu with system loading $S = 1 \angle 41^\circ$ pu, where 1.0 pu represents the rated output KVA of the machine. Figures 9 and 10 shown the same feedback system at lighter machine loads. With $S = 0.25 \angle 5^\circ$, the low frequency loci has shifted to the right, particularly at high machine speeds. With load further reduced, the locus will shift completely into the RHP, as shown in Figure 10. In these cases, the high frequency locus begins well into the LHP and moves into the RHP at very high gains.

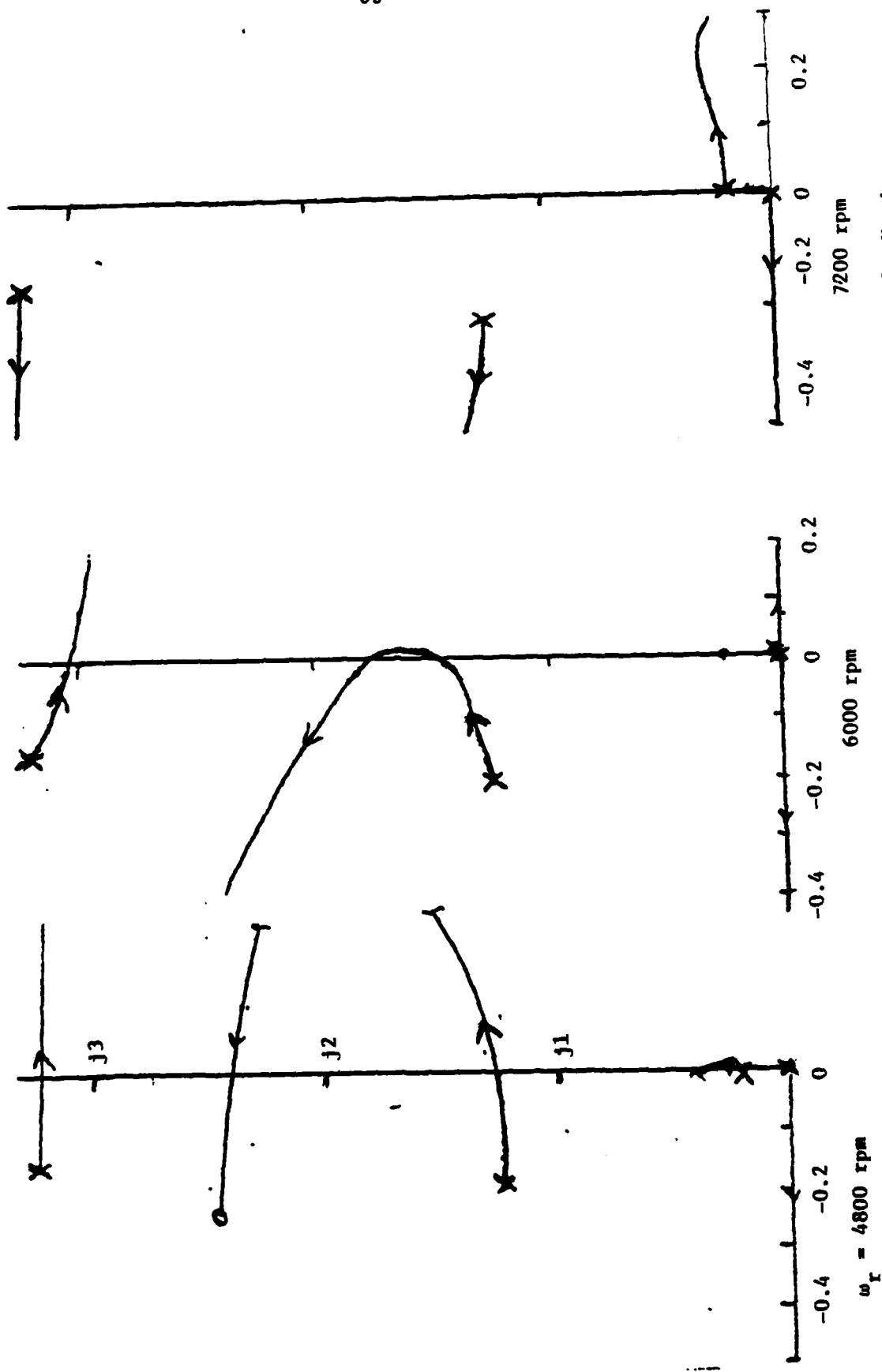


Figure 7. Closed loop pole movement with increasing integrator gain. No state feedback, Light load condition, $S = 0.1 \angle 5^\circ$ pu.

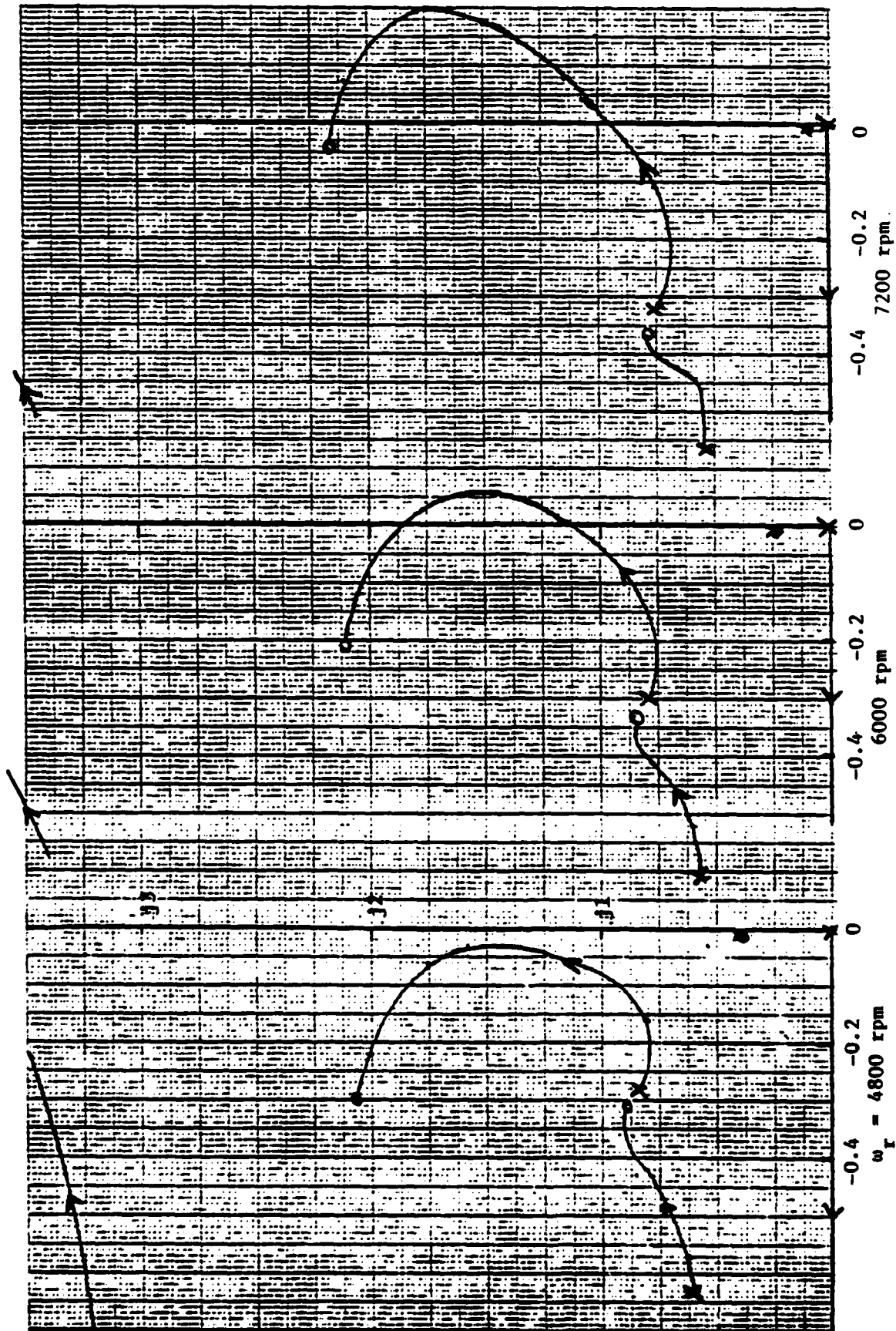


Figure 8. Closed loop pole movement with increasing integrator gain. Rotor current feedback $C_1 = 2.0$. Full load condition: $S = 1.0$ pu.

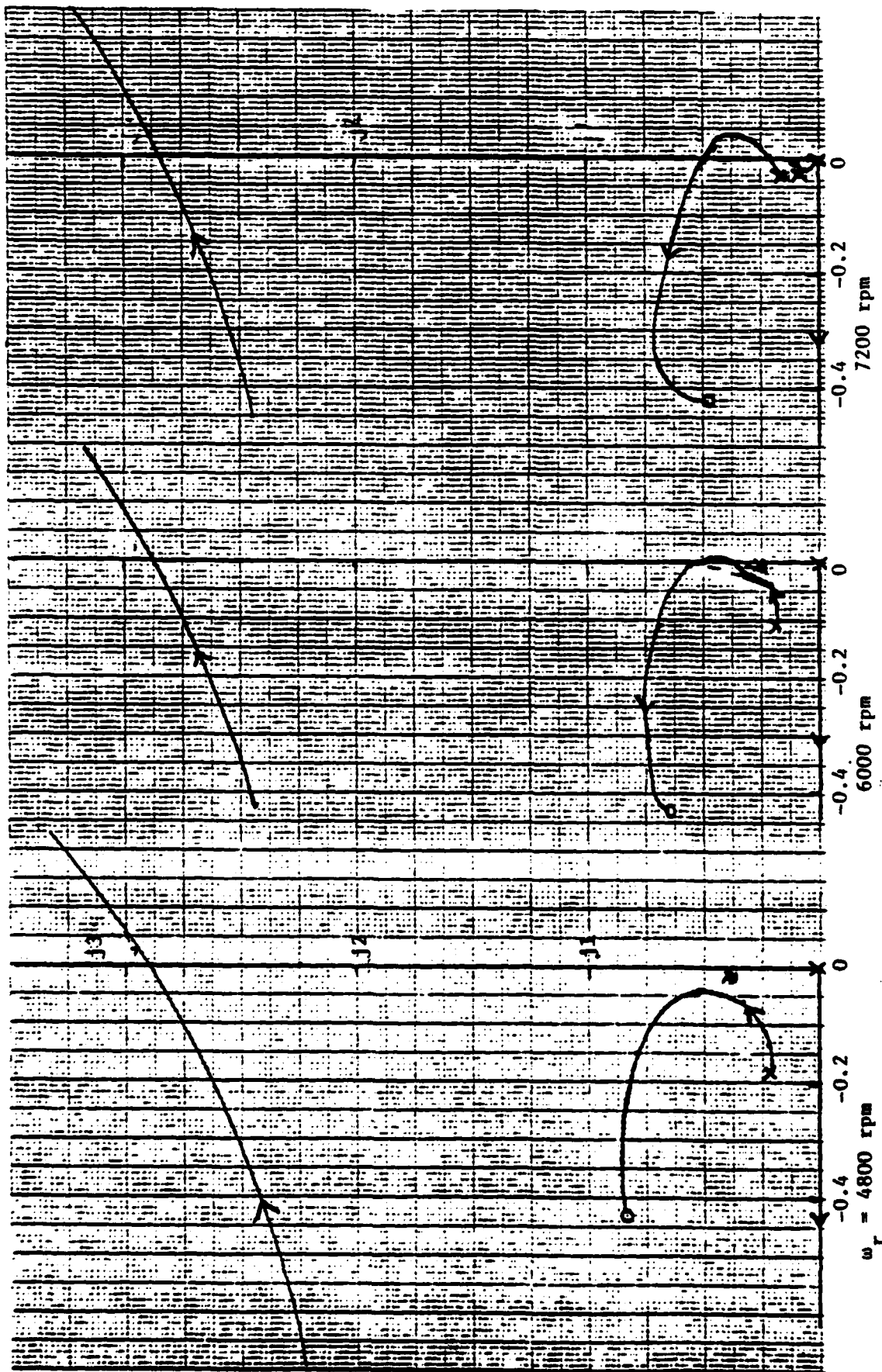


Figure 9. Closed loop pole movement with increasing integrator gain. Rotor current feedback $C_1 = 2.0$. Medium load condition: $S = 0.25 \angle 5^\circ$ pu.

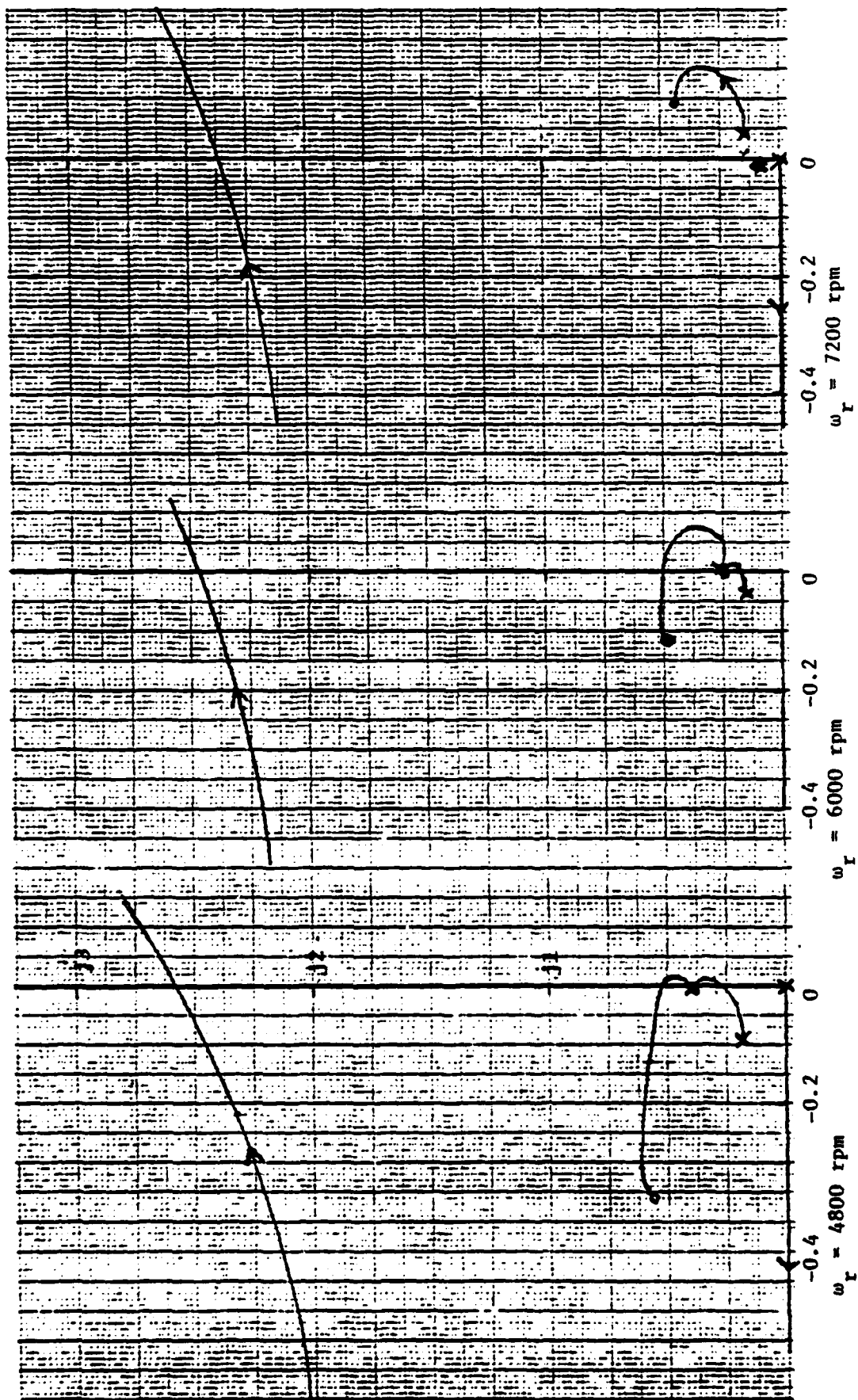


Figure 10. Closed loop pole movement with increasing integrator gain. Rotor current feedback $C_1 = 2.0$.
Light load condition: $S = 0.1 \angle 5^\circ$ pu.

The system stability will be studied at light load. $S = 0.1\angle 5^\circ$ is chosen, as damping is reduced as the load power factor angle is reduced. Note that, with capacitance, the generator will be operating with low power factor leading current with this load. Figure 11 shows the open loop pole movement for the system as C_1 is varied from 0 to 1 pu. This result shows that resistance simulation alone will not stabilize the system at this load level.

Next studied was the feedback equation

$$\begin{bmatrix} v_{df} \\ v_{qf} \end{bmatrix} = \begin{bmatrix} v_{df} \\ 0 \end{bmatrix} - \begin{bmatrix} C_1 & -C_2 \\ C_2 & C_1 \end{bmatrix} \begin{bmatrix} i_{df} \\ i_{qf} \end{bmatrix} \quad (26)$$

where C_1 is the resistance simulation. C_2 can be expected to provide some level of frequency shifting of the open loop poles [3].

Figure 12 shows the effect of C_2 on the open loop poles of the system. It can be seen that increased C_2 will move the unstable pole into the LHP while causing the previously well damped pole to move toward the RHP. The best response was obtained with $C_1 = 0.2$, $C_2 = 2.25$. The root locus plot with $S = 0.1\angle 5^\circ$ is shown in Figure 13. While stable operation can be obtained at this loading the response time would be slow, particularly at high speed. Figure 14 shows the result of the increased load, with $S = 0.2\angle 5^\circ$. At this load level, stable operation with good response can be obtained. Note that, with $C_1 = 0.2$ and $C_2 = 2.25$, the locus of the high frequency pole initially breaks to the left, while the locus of the low frequency poles breaks to the right. As a result, the placement of the high frequency open loop pole can be much closer to the $j\omega$ axis the placement of the low frequency open loop pole.

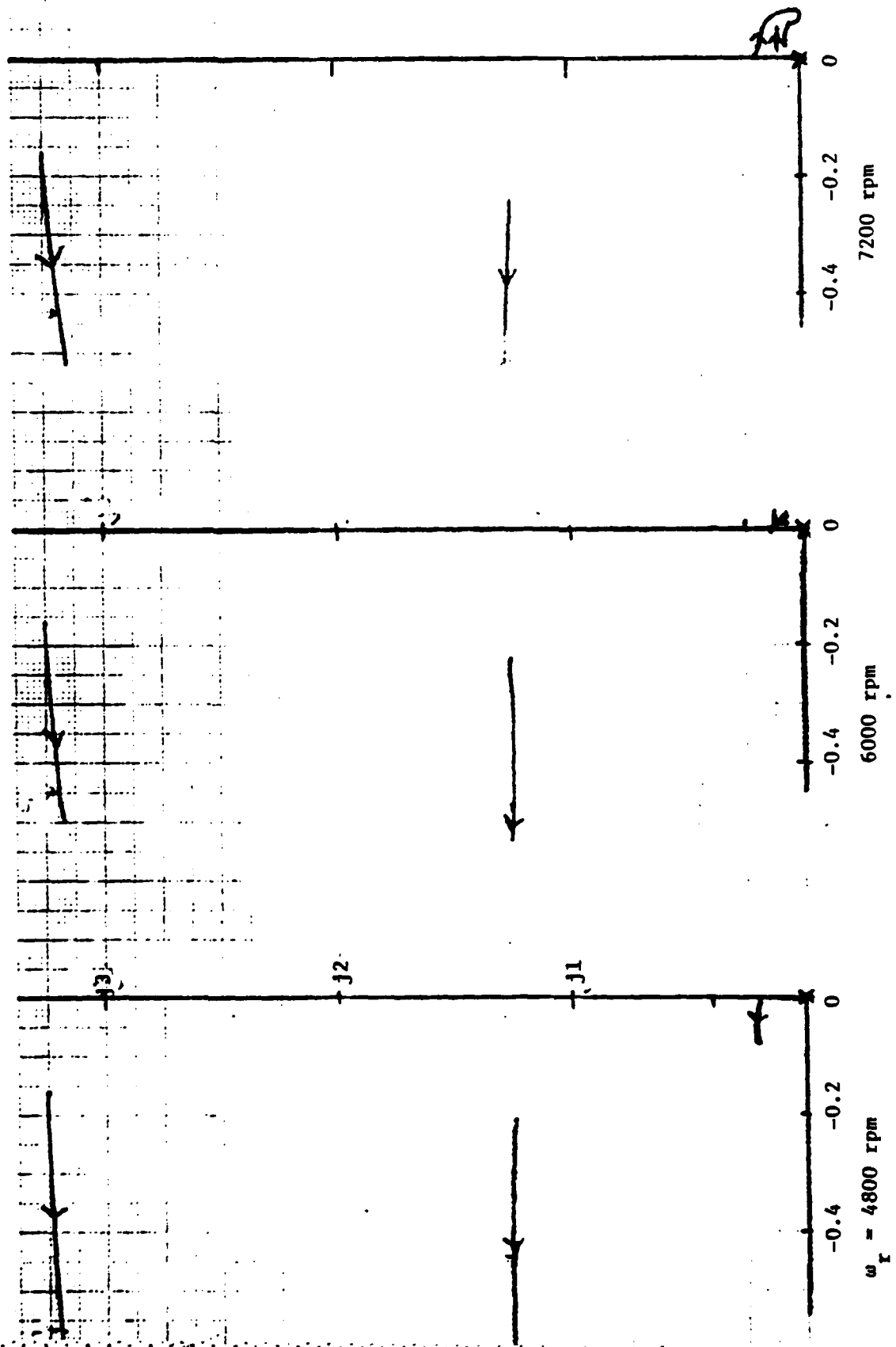


Figure 11. Open loop pole movement with variation rotor feedback parameter C_1 . C_1 varied from 0.0 to 1.0 with no other feedback.

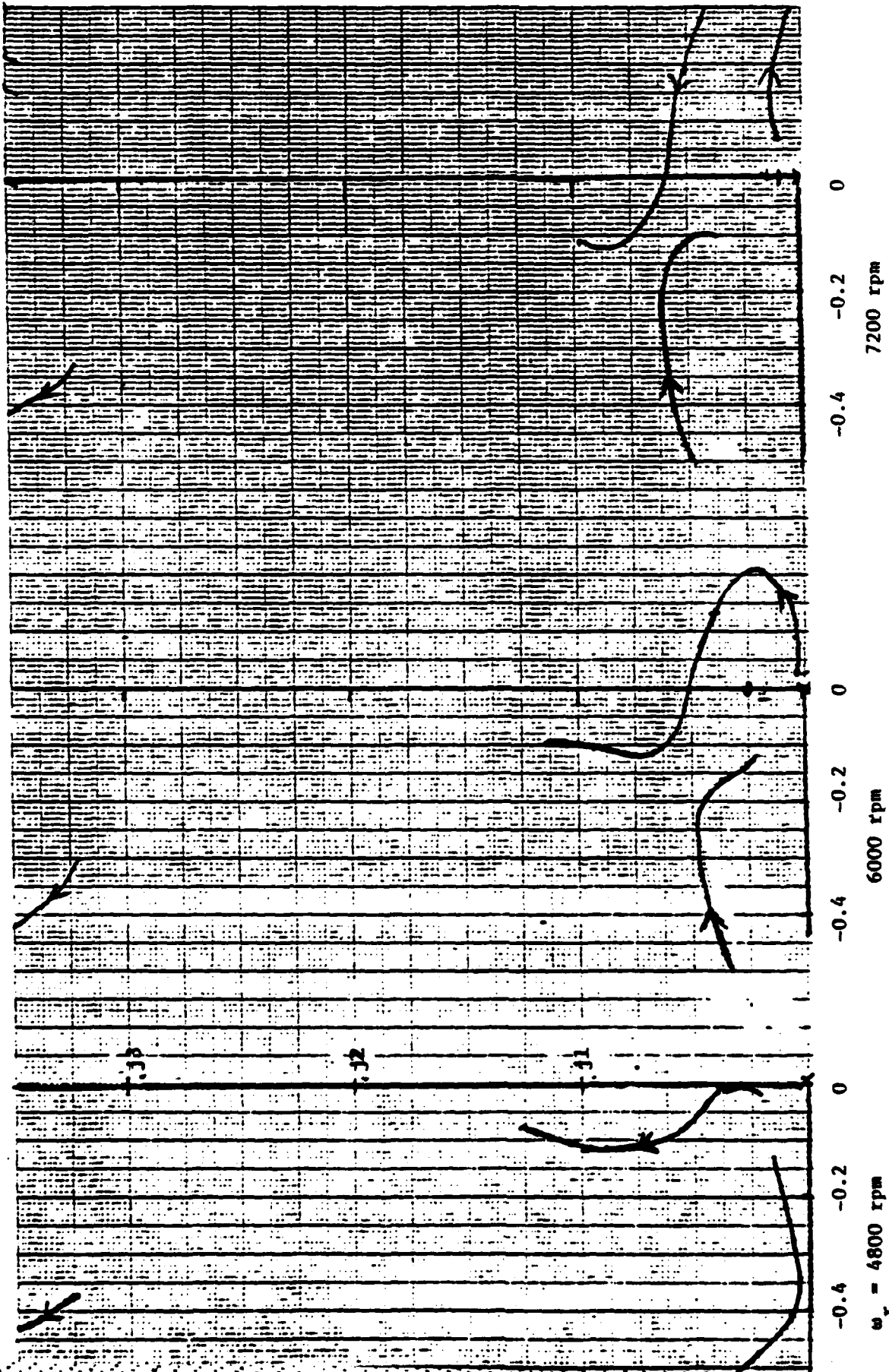


Figure 12. Open loop pole movement with variation of rotor feedback parameter C_2 . C_2 increased from 0 to 2.50 with $C_1 = 0.2$.

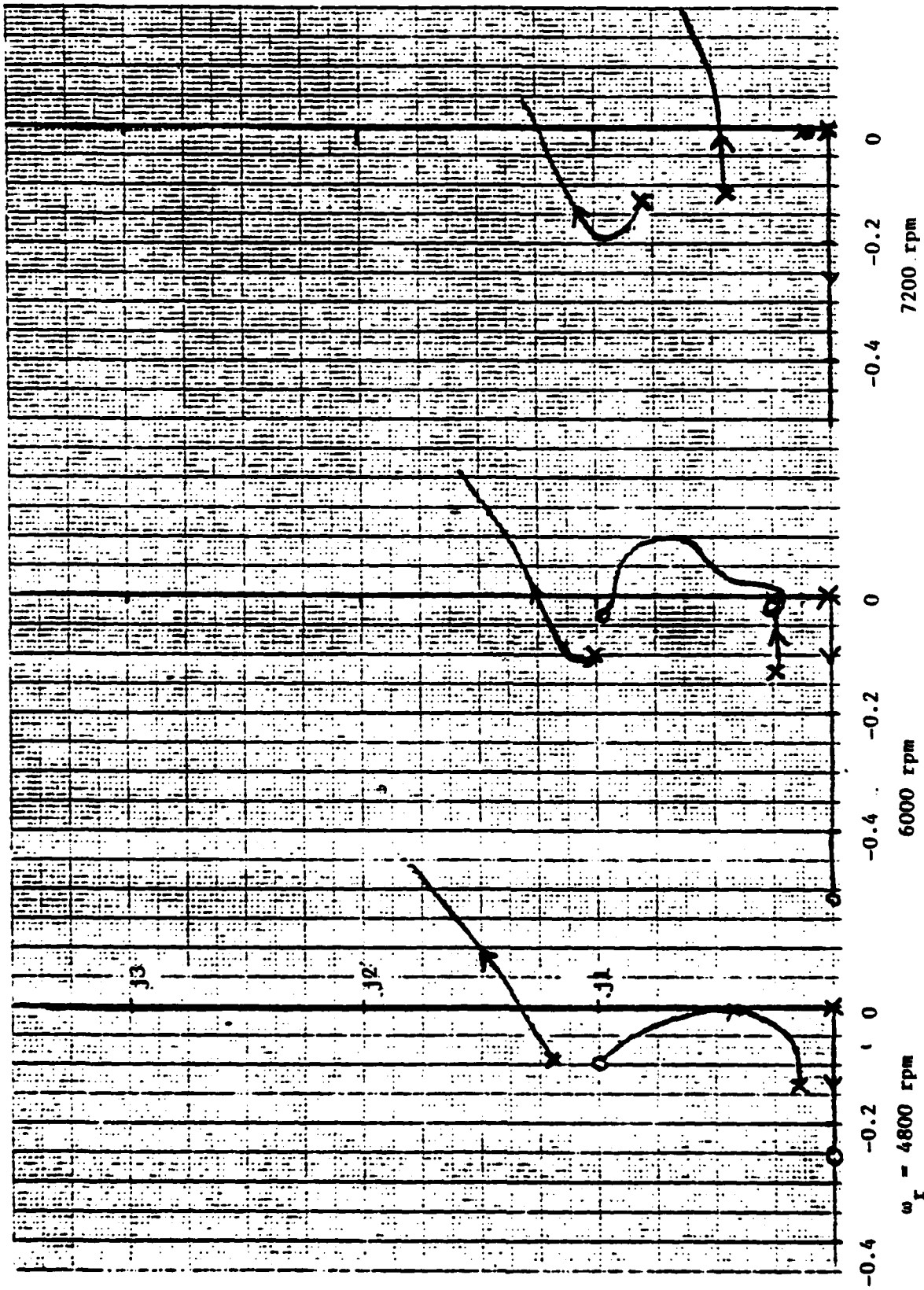


Figure 13. Closed loop pole movement with increasing integrator gain. Rotor feedback parameters $C_1 = 0.2$, $C_2 = 2.25$. System loading $S = 0.115$ pu.

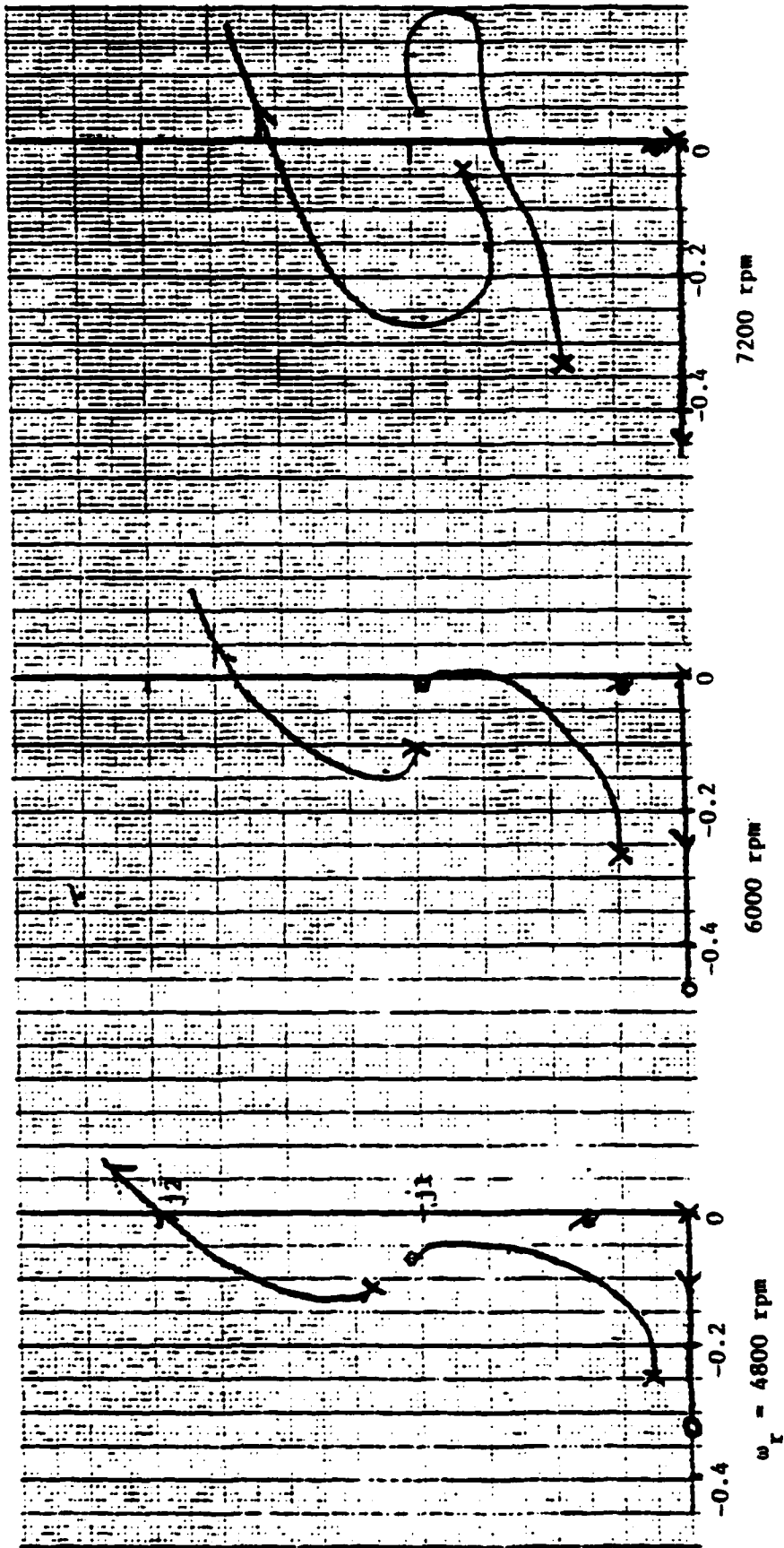


Figure 14. Closed loop pole movement with increasing integrator gain. Rotor feedback parameters $C_1 = 0.2$, $C_2 = 2.25$. System loading at $S = 0.25$ pu.

Due to the poor response at low power levels, the effect of adding feedback from the output of the generator was studied. A number of feedback possibilities were considered. It was considered that feedback of the d and q axis output quantities would be more difficult to implement than feedback of other quantities such as rms current, power, VARS. From the feedback strategies studied, the most successful were:

a) Feedback of capacitor d and q axis current

$$\begin{bmatrix} v_{df} \\ v_{qf} \end{bmatrix} = \begin{bmatrix} v_{df} \\ 0 \end{bmatrix} - \begin{bmatrix} C_1 & -C_2 \\ C_2 & C_1 \end{bmatrix} \begin{bmatrix} i_{df} \\ i_{qf} \end{bmatrix} + C_3 \begin{bmatrix} i_{dL} - i_{ds} \\ i_{qL} - i_{qs} \end{bmatrix} \quad (27)$$

b) Feedback of machine output current

$$\begin{bmatrix} v_{df} \\ v_{qf} \end{bmatrix} = \begin{bmatrix} v_{df} \\ 0 \end{bmatrix} - \begin{bmatrix} C_1 & -C_2 \\ C_2 & C_1 \end{bmatrix} \begin{bmatrix} i_{df} \\ i_{qf} \end{bmatrix} + C_3 \begin{bmatrix} i_{ds} \\ i_{qs} \end{bmatrix} \quad (28)$$

c) Feedback of rms output current.

The rms current is

$$I_s = (i_{ds}^2 + i_{qs}^2)^{1/2} \quad (29)$$

and the incremental value is

$$I_{sl} = \frac{i_{dso}}{I_{so}} i_{dsl} + \frac{i_{qso}}{I_{so}} i_{qsl} \quad (30)$$

The feedback equation studied is

$$\begin{bmatrix} v_{df} \\ v_{qf} \end{bmatrix} = \begin{bmatrix} v_{df} \\ 0 \end{bmatrix} - \begin{bmatrix} C_1 & -C_2 \\ C_2 & C_1 \end{bmatrix} \begin{bmatrix} i_{ds} \\ i_{qf} \end{bmatrix} + \begin{bmatrix} C_3 \\ C_3 \end{bmatrix} I_s$$

d) Feedback of output power.

The output power is

$$P = -[v_{ds} i_{ds} + v_{qs} i_{qs}] \quad (32)$$

with incremented power

$$P_1 = -v_{dso} i_{ds1} - i_{dso} v_{ds1} - v_{qso} i_{qs1} - i_{qso} v_{qs1} \quad (33)$$

For feedback to the d axis,

$$\begin{bmatrix} v_{df} \\ v_{qf} \end{bmatrix} = \begin{bmatrix} v_{df} \\ 0 \end{bmatrix} - \begin{bmatrix} C_1 & -C_2 \\ C_2 & C_1 \end{bmatrix} \begin{bmatrix} i_{df} \\ i_{qf} \end{bmatrix} - \begin{bmatrix} C_3 \\ 0 \end{bmatrix} P \quad (34)$$

Figure 15 shows a comparison of the open loop poles for feedback types a (dq axis capacitor currents) and c (output current magnitude). The field feedback remains at $C_1 = 0.2$ and $C_2 = 2.25$ pu.

Both yield increases in damping at the low frequency eigenvalue, and cause losses in damping at the high frequency eigenvalue. Figure 16 shows the closed loop pole migration for a similar case of capacitor current feedback. The locus diagrams are located well into the left half plane and stable operation with good response is obtained. The dominant eigenvalues at integrator gain of $G_1 = 200$ pu are shown in Table 2.

A study of power feedback (d) is shown in Figure 17. These loci are, for the most part, similar to those seen in Figure 16, and will provide stability with good response with the proper choice of gain. Table 3 lists the dominant eigenvalues for an integrator gain of 200 pu.

It is therefore possible to stabilize the system at light loads by including feedback of an output quantity. Therefore the option of providing output capacitors permanently connected to the generator would appear to be feasible, and should be considered in the design of a CDFM generator system.

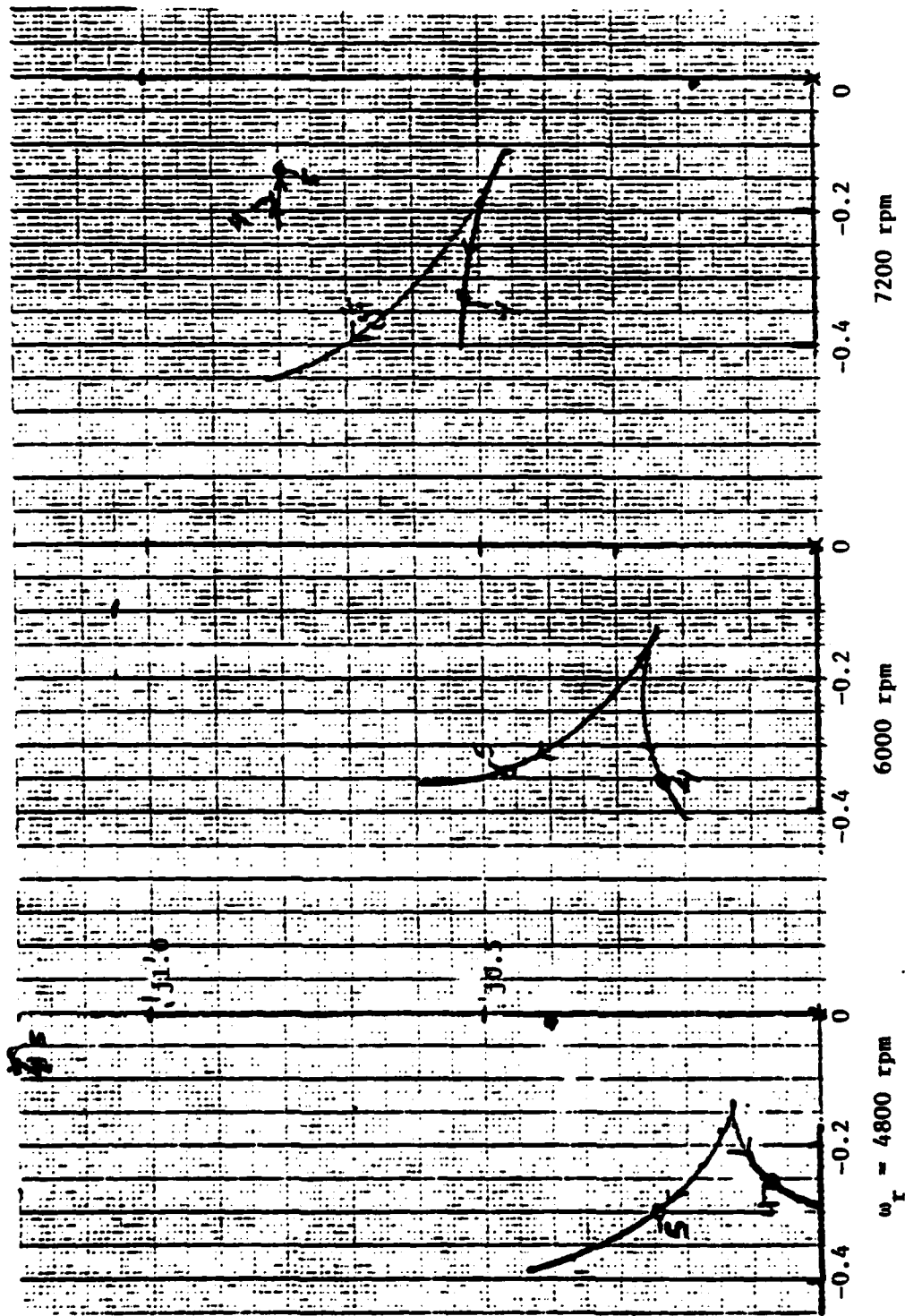


Figure 15. Open loop system poles with variation of feedback of stator quantities.
 Case 4: feedback of rms stator current. Case 5: feedback of d and q axis capacitor currents. In both cases, the stator current feedback parameter C_3 was varied from 0 to 1.8, with rotor current feedback parameters $C_1 = 0.2$ and $C_2 = 2.25$.

TABLE 2

Figure 16. Eigenvalue location at gain of 200 pu.

speed eigenvalues	4800 rpm	6000 rpm	7200 rpm
	-.16	-.12	-.09
	-.33 \pm j.31	-.26 \pm j.44	-.22 \pm j.60
	-.12 \pm j.88	-.12 \pm j.84	-.12 \pm j.76

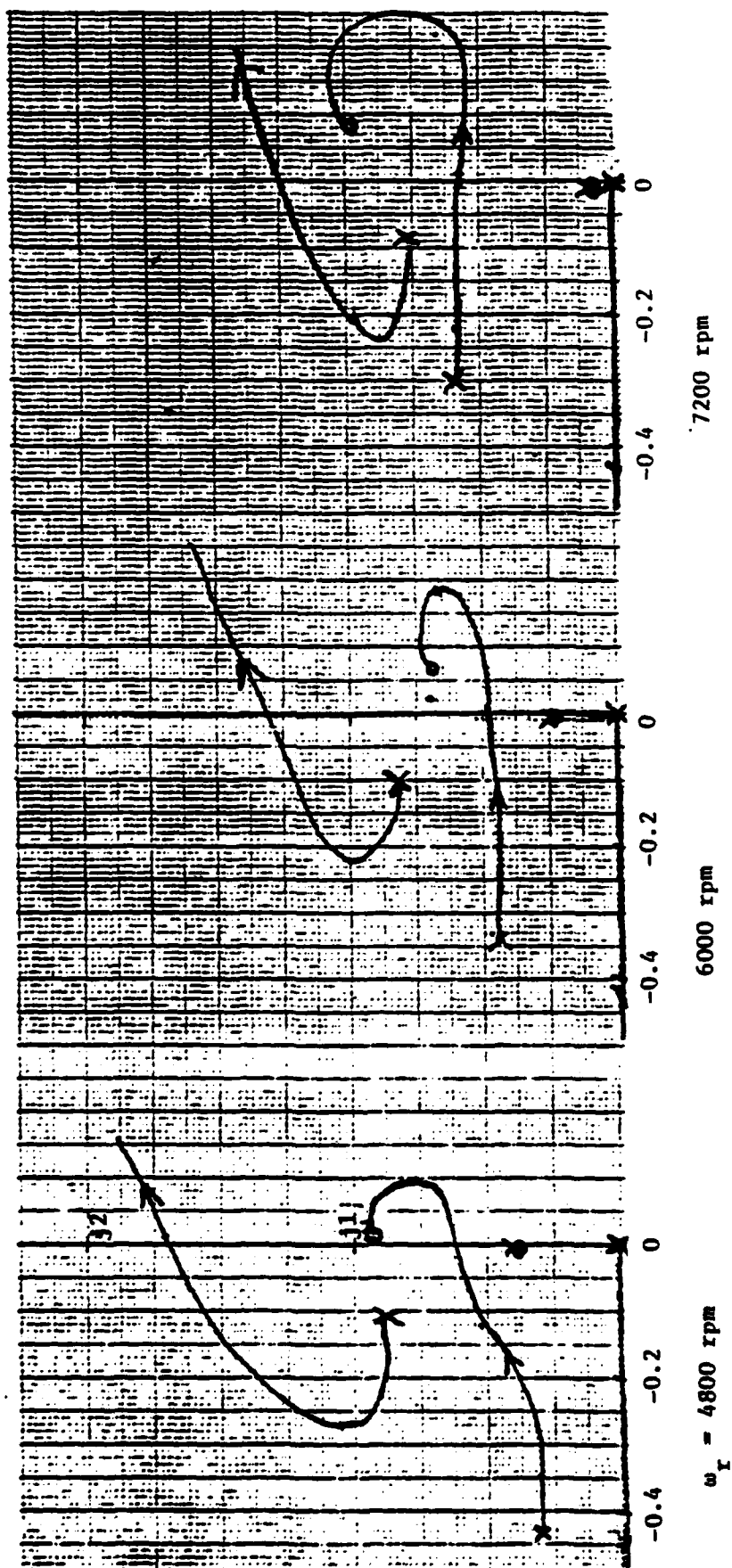


Figure 16. Closed loop pole movement with integrator gain. Rotor state feedback parameters $C_1 = 0.2$ and $C_2 = 2.5\omega_r$. Feedback of d and q axis capacitor currents with gain $C_3 = 0.6$.

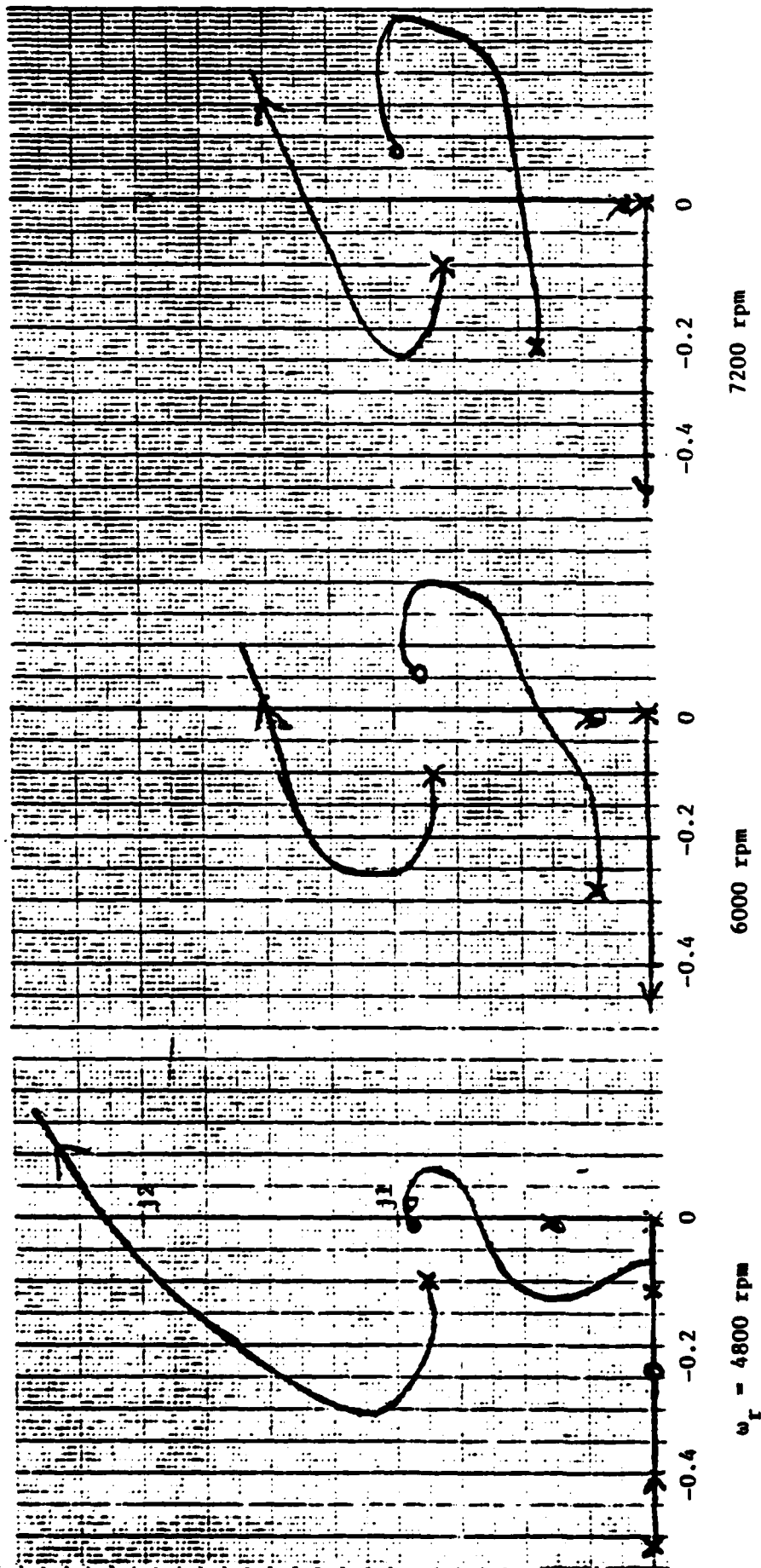


Figure 17. Closed loop pole movement with integrator gain. Rotor state feedback parameter $C_1 = 0.2$ and $C_2 = 2.5\omega_r$. Feedback of stator power with gain $C_3 = 0.6$.

TABLE 3

speed eigenvalues	4800 rpm	6000 rpm	7200 rpm
	-.40	-.29	-.14
	$-.10 \pm j.19$	$-.12 \pm j.25$	$-.13 \pm j.44$
	$-.11 \pm j.89$	$-.12 \pm j.85$	$-.12 \pm j.80$

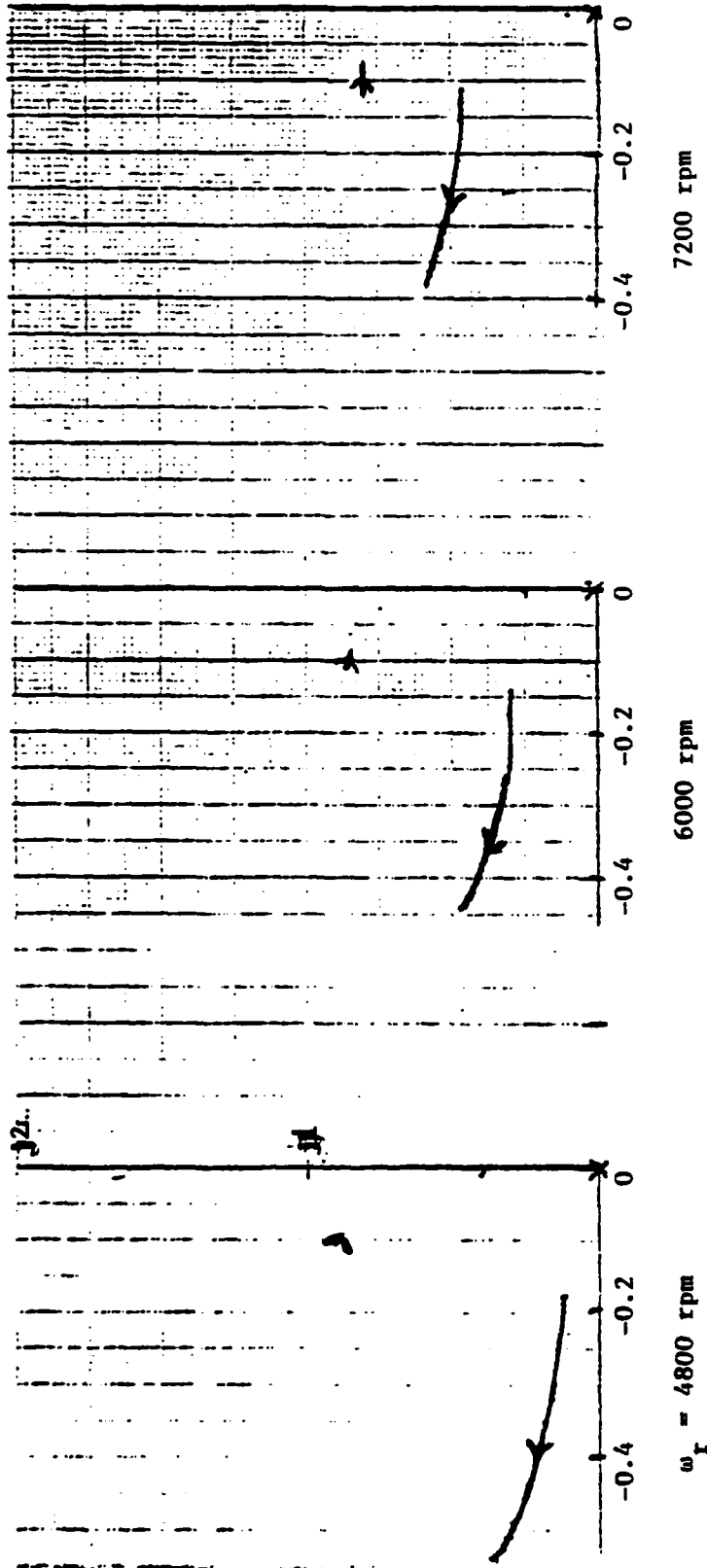


Figure 18. Open loop system poles with variation of feedback of stator currents. Stator current feedback parameter C_3 varied from 0.0 to 0.9. Field current feedback parameter $C_1 = 0.6$, $C_2 = 2.5\omega_r$.

Conclusions

This project considers two aspects of the control of cascaded doubly fed machine (CDFM) generator systems. In the first step, the controllability of the system in the supersynchronous operating mode was considered. The results show that the supersynchronous mode exhibits similar characteristics to the subsynchronous mode, which was considered during an earlier project. The supersynchronous mode exhibits certain characteristics which could be undesirable in systems requiring larger speed ranges than have been considered here.

The second step of the research considered the effect of shunt capacitance connected at the generator output, with permanently connected capacitors. The results show that stability and good response can be provided with field current feedback except at light load conditions. At light loads, stability and good response can be attained by including feedback of a generator output quantity. Of the options examined, feedback of the output power would appear to be the most easily implemented system. The results of this step show that permanently connected capacitors should be considered as a source of excitation for a CDFM generator system.

References

1. T.H. Ortmeyer and W.U. Borger, "Brushless Generation with Cascaded Doubly Fed Machines," Proceedings of the IEEE 1983 National Aerospace and Electronics Conference, Dayton, Ohio, pp. 1420-1425.
2. T.H. Ortmeyer, "Negative Frequency Aspects of Doubly Fed Machine Analysis," Proc. IEEE Vol. 71, No. 8, August, 1983, p. 1017.
3. T.H. Ortmeyer and W.U. Borger, "Control of Cascaded Doubly Fed Machines for Generator Applications," IEEE Trans. Vol. PAS-103, No. 9, September, 1984, pp. 2564-2571.
4. J.A. Weimer and T.H. Ortmeyer, "Experimental Cascaded Doubly Fed Variable Speed Constant Frequency Generator System," Proceedings of the IEEE 1984 National Aerospace and Electronics Conference, Dayton, Ohio, pp. 444-451.
5. T.H. Ortmeyer and J.A. Weimer, "Implementation of CDFM Generator Control," Submitted to IEEE Power Engineering Society.
6. A.E. Fitzgerald and C. Kingsley, Jr. Electric Machinery, 2nd edition, 1961. New York: McGraw Hill.

Appendix 1

Per Unit System

The per unit system used is:

Base current = machine rated rms phase current

Base Voltage = machine rated rms volts

Base power = machine rated volt-amps

Base Frequency = machine rated output frequency

The other bases follow from these definitions. The analysis and simulations were conducted on the output machine base. The base of the s-plane operator is $2\pi \times$ frequency base.

Appendix 2

Analysis and Simulation Program Listings

Step 1


```

0051 A(2.0)=LF
0052 A(3.0)=LF
0053 A(1.3)=LM
0054 A(1.4)=LM
0055 A(1.1)=L4
0056 A(4.2)=LM
0057 A(3.5)= -LA*CON
0058 A(4.5)= -LA*CON
0059 A(5.3)= -LA*CON
0060 A(5.4)= -LA*CON
0061 A(1.1)= -W*LM
0062 A(1.2)= -W*LM*(LS+LL)
0063 A(1.3)= -W*LM
0064 A(2.1)= WEU*(LS+LL)
0065 A(2.2)= W*LM
0066 A(2.3)= WEU*LM
0067 A(1.2)= -W*LM
0068 A(1.3)= W*LM
0069 A(1.4)= -(W*LM+W*LM*LA*CON)
0070 A(3.5)= WEU*LM
0071 A(4.1)= W*LM
0072 A(4.3)= W*LM*LA*CON
0073 A(4.4)= W*LM
0074 A(4.5)= -WEU*LM*CON
0075 A(5.4)= W*LM*CON
0076 A(5.5)= W*LM
0077 A(5.6)= -W*LM*LF -C2
0078 A(6.6)= W*LM
0079 A(6.5)= W*LM*LF+C2
0080 A(6.3)= -W*LM
0081 IYR = (V0-HS*IXS+W*LM*LS*IXS)/(-W*LM)
0082 IYR = (-HS*IXS - W*LM*LS*IXS)/(W*LM)
0083 IXF = (-W*LM*IXS-(W*LM*LA*CON+W*LM*LA)*IXR-(H*RA)*IYR)/
      (-W*LM*LA*CON)
0084 IYF = (-H*RA)*IXR+W*LM*IXS+(W*LM*LA*CON+W*LM*LA)*IYR/(W*LM*LA)
0085 VXF = (H*CI)*IXF+CON*W*LM*IXR-(W*LM*LF+C2)*IYF
0086 VYF = (H*CI)*IYF-W*LM*IXR+(W*LM*LF+C2)*IXF
0087 VDF = DSUP(VXF*VXF+VYF*VYF)
0088 DSH = VXF/VDF
0089 DSH = (VYF/VDF)*CON
0090 A(7.1)= H*DSH + W*LM*LS*DSH
0091 A(7.2)= H*DSH - W*LM*LS*DSH
0092 A(7.3)= WEU*LM*DSH
0093 A(7.4)= -WEU*LM*DSH
0094 A(7.1)= LS*DSH
0095 A(7.2)= LS*DSH
0096 A(7.3)= LM*DSH
0097 A(7.4)= LM*DSH
0098 A(7.7)= W*DSH
0099 A(5.7)= -G1
0100 DO 13 J=1,N
0101 DO 13 K=1,N
0102 A(J,K) = -A(J,K)
0103 W*LM*(5.140) 61.W*LM

```

```

0104 IF (DASS(5,20).LT.0.10-4) GOTO 80
0105 CALL F15/F(A,4,M,N,G,RND,ALFA,HETA,Z,N,W,K,KER)
0106 IF (MFR.GT.125) GOTO 50
0107 140 F0=MAT(20X,012.4,10X,010.4)
0108 10 12 J=1,5
0109 ALFA(J) = ALFA(J) / HETA(J)
0110 WRITE(6,160) ALFA(J)
0111 160 FORMAT(40X,2(10X,012.5))
0112 GOTO 41
0113 CONTINUE
0114 10 12 JPR=1,7
0115 A(JPR,6)=A(JPR,7)
0116 12 JPR=6)=A(JPR,7)
0117 10 13 JPR=1,6
0118 A(JPR,6)=A(7,JPR)
0119 13 JPR)=A(7,JPR)
0120 CALL E10/F(A,6,4,M,N,1,KND,ALFA,HETA,Z,N,W,K,KER)
0121 IF (MFR.GT.125) GOTO 50
0122 JME=1
0123 10 14 J=1,M2
0124 ALFA(J)=ALFA(J)/HETA(J)
0125 14 WRITE(6,160) ALFA(J)
0126 14 CONTINUE
0127 14 J=61+4.0
0128 CONTINUE
0129 IF (SHAFT.GT.SPMAX) GOTO 17
0130 SHAFT = SHAFT + JSP
0131 GOTO 16
0132 CONTINUE
0133 STOP
0134 50 WRITE(6,150) KER
0135 150 FORMAT(10X,14)
0136 STOP
0137 END

```

OPTIONS IN EFFECT NOFORM,IO,FACIOIC,SOURCE,NOLIST,NOUECK,LOAD,NOMAP,NOTEST
 OPTIONS IN EFFECT NAME = MAIN LINECNT = 56
 STATISTICS SOURCE STATEMENTS = 137,PROGRAM SIZE = 001402
 STATISTICS NO DIAGNOSTICS GENERATED

/DATA

00CF00 BYTES USED

EXECUTION RESIDS

MS = .20000-01PR = .25900-01LS = 4.0000

MA = .40000-02 OF = 10000-01

LM = 4.000

LM = 4.000

PI = 6.000

3.85


```

0001 IMPLICIT REAL*4 (A-H,L,I,O-Z)
0002 DIMENSION Y(7),W(7,4),C(24)
0003 EXTERNAL FCN
0004 COMMON /AL/ F1,XT,XN,VDF,FR,AR,SLIP,VDF,LS,LM,CND
0005 COMMON /AL4/ G10,G20,B30,B120,B130,B230,B10,B20,B30,B120,B130,B230
0006 COMMON /AL3/ N
0007 COMMON /AL2/
0008 CR5,CR6,XN,VDF5,I,G1,G2,V0,LT,LM,PHI1
0009 COMMON /AL1/ P2,LA,PF,LF,LAM,P2,WS,WE2,WS2,WE,CON
0010 REAL(5,100) TDEL,TFINAL
0011 WRITE(6,150) TDEL,TFINAL
150 FORMAT('TIME INCREMENT= ',F7.4,'FINAL TIME = ',F7.4)
0012 READ(5,100) MS,MW,LS,LM,LMP1
0013 READ(5,100) RA,RF,LA,LF,LAM,P2
0014 READ(5,100) VO,PO,UO,FO,SHAFT
0015 WRITE(6,110) MS,MW,LS,LM,LMP1
0016 WRITE(6,121) RA,RF,LA,LF,LAM,P2
0017 FORMAT(' ',F10.4,' ',F10.4,' ',F10.4,' ',F10.4,' ',F10.4,' ',F10.4)
0018 CRX,LF=,F10.4,' ',F10.4,' ',F10.4,' ',F10.4,' ',F10.4)
0019 WRITE(6,120) VO,PO,UO,FO,SHAFT
100 FORMAT(' ',F10.4)
0019 FORMAT(' ',F10.4,' ',F10.4,' ',F10.4,' ',F10.4,' ',F10.4)
0020 C'LM=,F10.4,' ',F10.4,' ',F10.4,' ',F10.4,' ',F10.4)
0021 FORMAT(' INITIAL CONDITIONS OUTPUT: V0= ',F7.3,'4X, 'PU= ',
CF7.4,'2X, 'G0= ',F7.3,'20X, 'FO= ',F7.2,'SHAFT SPEED= ',F10.2,
C' ')
0022 READ(5,100) DELV,DELN,DELP,DELX,G1,G2
0023 WRITE(6,130) DELV,DELN,DELP,DELX,G1,G2
130 FORMAT('STEP CHANGES: VOLTAGES= ',F7.3,'2X, 'SHAFT SPEED = ',
CF7.3,'2X, 'LOAD RESISTANCE= ',F7.3,'2X, 'LOAD REACTANCE= ',F7.3,
C'GAIN G1 = ',F7.3,'5X, 'G2= ',F7.3)
0025 READ(5,101) K
101 FORMAT(' ')
0026 WRITE(6,140) K
140 FORMAT('OK= ',I3,'4X, '(K=1 FOR PER UNIT OPERATION, '
C'K = 2 FOR DIMENSIONAL OPERATION)')
C CALCULATE GENERATOR CONSTANTS
0029 COST = 0.0
0030 K4 = 7
0031 TOL = 0.00001
0032 PA1 = 3.14159
0033 CO1 = 1.0
0034 K0 = 2.0*PA1*PI
0035 W0 = 30
0036 CR0 = 100./PA1
0037 IF (CR0.1) W0 = 1.
0038 IF (CR0.2) W0B = 1.
0039 AM = W0*LM
0040 RS = W0*LS
0041 AM = W0*LM
0042 = 0
0043 T = -2.0*TDEL
0044 V0ST = V0
0045 P0 = 1

```

DATE = TUE DEC 06, 1983

MAIN

DELTA = 2.0

FORTRAN IV G1

C CALCULATE INITIAL CONDITIONS

```

0046 PSN = SNAFT*PI/120.
0047 SPE = F*120./PI
0048 SLIP = (SPE-SNAFT)/SPE
0049 IX = -PI/VO
0050 IY = PI/VO
0051 IOR = IY*IX*IY*IY
0052 IF (IORS*.LT.0.001)N = 1
0053 WE = W0
0054 AS = SLIP*W0
0055 IF (AS*.LT.0.0) CON=-1.0
0056 WE2 = CO*SLIP*W0
0057 AS2 = WE2-(PI2/PI)*(WE-WS)
0058 IX5 = IX
0059 WE0 = WE
0060 WE20 = WE2
0061 AS20 = AS2
0062 AS0 = AS
0063 IY5 = IY
0064 IYR = (VO-PS*IXS+WE0*LS*IYS)/(-WE0*LM)
0065 IXR = (-PS*IYS-WE0*LS*IXS)/(WE0*LM)
0066 IXF = (-WS0*LM*IXS-(WS0*LM*CON+WE20*LA)*IXR-(WR+RA)*IYR)/
      C (-WE20*LM*CON)
      C IYF = (-WR+RA)*IXR+WS0*LM*IYS+(WS0*LM*CON+WE20*LA)*IYR
      C /(-E20*LM)
0067 VXF = PI*IXF+CON*WS20*LM*IYR-WS20*LF*IYF
0068 VYF = PI*IYF-WS20*LM*IXR+WS20*LF*IXF
0069 VDF = DSORT(VXF*VXF+VYF*VYF)
0070 VUF = 0.
0071 A = VXF/VDF
0072 B = VYF/VDF
0073 Y(2) = IXR+A*IYR+H*CON
0074 Y(5) = -IXR+B*CON+IYH*A
0075 Y(1) = IXR+A*IYR+CON
0076 Y(4) = -IXR+B*CON+IYH*A
0077 Y(3) = IXF+A*IYF+B
0078 Y(6) = -H*IXF+A*IYF
0079 Y(7) = VDF
0080 *WRITE (999) Y(1),Y(2),Y(3),Y(4),Y(5),Y(6),Y(7)
0081 *RITE (9,110) IYR,IXR,IYF,IXF,VYF,VXF
0082 *DO=(LS*(LP+LA)*LF-LAM*LAM*LS-LM*LM*LF)/WOB
0083 *10=(LR*LA)*LF-LAM*LAM)/RD
0084 *20=(LS*LF)/RD
0085 *30=(LS*(LM+LA)-LM*LM)/BD
0086 *120=(LM*LF)/BU
0087 *130=(LM*LAM)/BU
0088 *230=(LS*LAM)/BU
0089 *10=h10
0090 *20=h20
0091 *30=h30
0092 *120=h120
0093 *130=CO*H130
0094 *230=CO*H230
0095 IF (H.EQ.0) GO TO 40
0096

```

```

0097      M2 = M2
0098      M4 = M4
0099      Z = 0.
0100      Z4 = M0/VLR
0101      ZT = M5
0102      ZT = M5
0103      GO TO 60
0104      Z = P0/IOSU
0105      X = 00/IOSU
0106      ZY = P5+X
0107      ZT = M5+X
0108      CONTINUE
0109      LT = XT/40
0110      WRITE (6,102)
0111      FORMAT (
102      C 'OUTPUT',6X, 'ANGLE',
          '1',4X, 'TIME',7X, 'OUTPUT',6X,
          9X, 'IDS', 9X, 'IDR', 9X, 'IOS', 9X, 'IQR',
          9X, 'VDR', 9X, 'VDR',
          9X, 'VOLTAGE', 5X, 'CURRENT', 3X, 'VOUT TO VDR', 1X,
          C 'TO VDR')
          CALL WRIT (I,Y,K4)
          TEND = T+TDELTA
          CALL OVERK(K4,FCN,I,Y,TEND,TOL,KND,C,K4,W,KER)
          IF (KND-LT.0) GO TO 15
          IF (KER-GT.0) GO TO 15
          CALL WRIT (I,Y,K4)
          IF (TFND-LT.-.00005) GO TO 20
          INPUT CONDITIONS
          VOST = VOST + DELV
          SHAFT = SHAFT + DELN
          SLIP = (SPE-SHAFT)/SPE
          WS = SLIP
          WE2 = CON*SLIP*W0
          WS2 = WE2-(P2/P1)*(WE-WS)
          IF (DELX-GT.0.001.0P.0.001) GO TO 60
          GO TO 61
          IF (N.F2.0) GO TO 61
          I = 0
          M2 = M2P
          M4 = M4P
          CONTINUE
          ZT = ZT + DELX
          ZT = ZT + DELX
          IELO = I + TDELTA
          ZM = M3+1
          CALL OVERK(K4,FCN,I,Y,TEND,TOL,KND,C, K4,W,KER)
          IF (KND-LT.0) GO TO 15
          IF (KER-GT.0) GO TO 15
          CALL WRIT (I,Y,K4)
          IF (TFND-LT.FINAL) GO TO 25
          STOP
          WRITE (6,160) KND,KER
          FORMAT ('ERROR-KND=,12,KER=,12')
          STOP
160
0112
0113
0114
0115
0116
0117
0118
0119
0120
0121
0122
0123
0124
0125
0126
0127
0128
0129
0130
0131
0132
0133
0134
0135
0136
0137
0138
0139
0140
0141
0142
0143
0144

```


WRITE

```

0001 SUBROUTINE WRITE(I,Y,K4)
0002 IMPLICIT REAL*8 (A-H,L,10-2)
0003 DIMENSION Y(K4)
0004 COMMON /BL/AT,AM,VDF,PH,XM,SLIP,VDF,LS,LM,CMD
0005 COMMON /BL3/ I
0006 COMMON /BL2/
0007 CAS,ES,XOH,VOST,G1,G2,VO,LI,LM,PHI1
0008 IA=EOSRT(Y(1)*Y(1)+Y(4)*Y(4))
0009 IF (PH.EQ.1) GO TO 10
0010 PHI1=DATAN2(Y(4),Y(1))*CMD
0011 GO TO 11
0012 PHI1=0.
0013 CONTINUE
0014 WRITE(6,170) I,VO,IA,PHI1,Y(1),Y(2),Y(3),Y(4),Y(5),Y(6),Y(7)
0015 FORMAT(1,3(F9.4,3X),2(F7.2,5X),6(F9.4,3X))
0016 RETURN
0017 END

```

OPTIONS IN EFFECT NOTEMP,IO,EMCOIC,SOURCE,NOLIST,NODECK,LOAD,NOMAP,NOTEST

OPTIONS IN EFFECT NAME = WRITE, LINECNT = 56

STATISTICS SOURCE STATEMENTS = 16, PROGRAM SIZE = 000344

STATISTICS NO DIAGNOSTICS GENERATED

STATISTICS NO DIAGNOSTICS THIS STEP

4.15

/DATA

009470 BYTES USED

EXECUTION BEGINS

TIME INCREMENT= 0.0020 FINAL TIME = 0.7000

Analysis and Simulation Program Listings

Step 2


```

0041      IF (C1) THEN
0042      IF (C2) THEN
0043      IF (C3) THEN
0044      IF (C4) THEN
0045      IF (C5) THEN
0046      IF (C6) THEN
0047      IF (C7) THEN
0048      IF (C8) THEN
0049      IF (C9) THEN
0050      IF (C10) THEN
0051      IF (C11) THEN
0052      IF (C12) THEN
0053      IF (C13) THEN
0054      IF (C14) THEN
0055      IF (C15) THEN
0056      IF (C16) THEN
0057      IF (C17) THEN
0058      IF (C18) THEN
0059      IF (C19) THEN
0060      IF (C20) THEN
0061      IF (C21) THEN
0062      IF (C22) THEN
0063      IF (C23) THEN
0064      IF (C24) THEN
0065      IF (C25) THEN
0066      IF (C26) THEN
0067      IF (C27) THEN
0068      IF (C28) THEN
0069      IF (C29) THEN
0070      IF (C30) THEN
0071      IF (C31) THEN
0072      IF (C32) THEN
0073      IF (C33) THEN
0074      IF (C34) THEN
0075      IF (C35) THEN
0076      IF (C36) THEN
0077      IF (C37) THEN
0078      IF (C38) THEN
0079      IF (C39) THEN
0080      IF (C40) THEN
0081      IF (C41) THEN
0082      IF (C42) THEN
0083      IF (C43) THEN
0084      IF (C44) THEN
0085      IF (C45) THEN
0086      IF (C46) THEN
0087      IF (C47) THEN
0088      IF (C48) THEN
0089      IF (C49) THEN
0090      IF (C50) THEN
0091      IF (C51) THEN

```


DISCLAIMER NOTICE

**THIS DOCUMENT IS BEST QUALITY
PRACTICABLE. THE COPY FURNISHED
TO DTIC CONTAINED A SIGNIFICANT
NUMBER OF PAGES WHICH DO NOT
REPRODUCE LEGIBLY.**

END

FILMED

3-85

DTIC